



A geometric optics based numerical method for high frequency electromagnetic fields computations near fold caustics - Part I

Jean-David Benamou, Olivier Lafitte, Rémi Sentis, Ian Sollicec

► To cite this version:

Jean-David Benamou, Olivier Lafitte, Rémi Sentis, Ian Sollicec. A geometric optics based numerical method for high frequency electromagnetic fields computations near fold caustics - Part I. [Research Report] RR-4422, INRIA. 2002. inria-00072166

HAL Id: inria-00072166

<https://hal.inria.fr/inria-00072166>

Submitted on 23 May 2006

HAL is a multi-disciplinary open access archive for the deposit and dissemination of scientific research documents, whether they are published or not. The documents may come from teaching and research institutions in France or abroad, or from public or private research centers.

L'archive ouverte pluridisciplinaire **HAL**, est destinée au dépôt et à la diffusion de documents scientifiques de niveau recherche, publiés ou non, émanant des établissements d'enseignement et de recherche français ou étrangers, des laboratoires publics ou privés.

***A geometric optics based numerical method for high
frequency electromagnetic fields computations near
fold caustics - Part I***

J.-D. Benamou, O. Lafitte, R. Sentis and I. Sollicc

N° 4422

mars 2002

THÈME 4



***apport
de recherche***



A geometric optics based numerical method for high frequency electromagnetic fields computations near fold caustics - Part I

J.-D. Benamou, O. Lafitte, R. Sentis and I. Sollic

Thème 4 — Simulation et optimisation
de systèmes complexes
Projet OTTO

Rapport de recherche n° 4422 — mars 2002 — 51 pages

Abstract: This paper presents an Eulerian numerical method for the computation of a bi-valued solution of Hamilton-Jacobi type equation in a particular geometric setting. More precisely we consider High Frequency electromagnetic fields in the vicinity of fold caustics.

Key-words: Hamilton-Jacobi, Hamiltonian System, Ray Tracing, Viscosity Solution, Upwind Scheme, Geometric Optics, Eave Equation, Laser, Plasma, Electromagnetism.

Une méthode de calcul de champs électromagnétiques hautes fréquences au voisinage de caustiques de type pli basée sur l'optique géométrique - Première partie

Résumé : Ce papier présente une méthode numérique Eulérienne pour le calcul de solutions bi-valuées d'équation de type Hamilton-Jacobi. Plus précisément nous considérons des champs électromagnétique hautes fréquences au voisinage de caustiques de type pli.

Mots-clés : Hamilton-Jacobi, Système Hamiltonien, Lancer de rayons, Solution de Viscosté, Schéma Décentrés, Optique Géométrique, Equation des Ondes, Laser, Plasma, Electromagnétisme

Introduction

We are concerned with the propagation of a laser wave in a material medium. A new and important application is the design of very high power laser devices such as the Laser MEGA-Joule (LMJ) in France or the National Ignition Facility (NIF) in the USA. The laser electromagnetic field can be accurately modeled and computed by the solution $A = A(X)$ of the following frequency wave equation [36]

$$\vec{\nabla}(\vec{\nabla} A) + k_0^2(1 - N)A + i\nu k_0 A = 0. \quad (1)$$

The space variable X belongs to \mathbf{R}^{d+1} ($d = 1$ in the sequel), $\vec{\nabla}$ is the gradient operator in \mathbf{R}^{d+1} , k_0 is the wave number of the laser wave in the vacuum, $N = N(X)$ is a given smooth positive function representing the adimensional electronic density of the material medium and ν a given positive function which characterizes the absorption coefficient of the laser energy by the material. We assume that $0 \leq N < 1$ since the laser wave cannot propagate in regions where $N \geq 1$. Equation (1) may be set in an unbounded domain with an incident known excitation A_{inc} . The equation is then complemented by or in a bounded domain with so-called radiation boundary conditions (or equivalent absorbing boundary conditions in a bounded domain) satisfied by $A - A_{inc}$. The definition of domain and boundary conditions are intimately linked with the problem of multi-valued geometric optics and are discussed below.

The W.K.B. approximation

The oscillatory behavior of the solution generally makes the numerical resolution of (1) too expensive even in two dimensions. Fortunately, the wave length $2\pi k_0^{-1}$ is less than $1\mu m$ and much smaller than the scale of the variations of N . It is therefore relevant to use a W.K.B. (high frequency) approximation of A [26]. Let us recall briefly the principle of this approximation before discussing numerical methods in this framework. The solution of (1) is a priori replaced by the following asymptotic expansion

$$A = (a + \frac{a_1}{ik_0} + \frac{a_2}{(ik_0)^2} + \dots) \exp(ik_0 \phi) \quad (2)$$

called the W.K.B. ansatz. At the leading significant orders, the equation (1) writes

$$\begin{aligned} 0 &= k_0^2 a \left[N - 1 + |\vec{\nabla} \phi|^2 \right] \\ &\quad - ik_0 \left[\nu a + 2 \vec{\nabla} a \cdot \vec{\nabla} \phi + a \vec{\nabla}(\vec{\nabla} \phi) \right] + \dots \end{aligned}$$

Thus, equating the coefficient of k_0^2 to zero, we get the so-called Eikonal equation for the phase ϕ

$$|\vec{\nabla} \phi|^2 = 1 - N \quad (3)$$

Setting $n(X) = \sqrt{1 - N(X)}$, we recover the usual geometric optics Eikonal equation with index of refraction n ($0 < n \leq 1$).

Furthermore, equating the coefficient of k_0 to zero leads to the transport equation satisfied by the first term of the amplitude, a

$$\nu a + 2 \vec{\nabla} a \vec{\nabla} \phi + a \vec{\nabla} \cdot (\vec{\nabla} \phi) = 0. \quad (4)$$

Note that the physically relevant quantity $E = |a|^2$, representing the laser energy, also satisfies a transport equation

$$\nu E + \vec{\nabla} \cdot (E \vec{\nabla} \phi) = 0, \quad (5)$$

νE being the absorbed laser energy.

This method of approximation of the solution of (1) is called geometrical optics. Several refinements of this theory such as Maslov theory (see [39] for an application of this theory in a geophysical context) or the geometrical theory of diffraction [16] for the diffraction of a wave by an object, have been proposed. The case of the solution near a caustic curve, our case, is treated in detail in [34]. To the best of our knowledge, existing numerical methods based on these mathematical tools use Lagrangian ray tracing solutions of (3). The goal of our study is to use Eulerian solutions of (3) in the resolution of (1).

We now analyse a solution of (3) in a very simple but relevant setting that convey a rough geometric picture of our problem. This solution is in particular bi-valued and defined in a domain bounded by a caustic curve, two general features of our problem.

Ray tracing - a Lagrangian method

This is best done using ray tracing which is the classical Lagrangian numerical method for solving (3). Basically, ray tracing relies on the remark that the integral curves of $\vec{\nabla} \phi$, called rays and denoted $Y(s)$ (i.e. $\frac{dY}{ds} = \vec{\nabla} \phi(Y(s))$ and s is a parameterization of the curve) are solutions of a simple system of ordinary differential equations (ODEs)

$$\frac{dY}{ds} = P(s), \quad \frac{dP}{ds} = \frac{1}{2} \vec{\nabla} (n^2)(Y(s)) \quad (6)$$

(set $P(s) = \vec{\nabla} \phi(Y(s))$ and use (3)). Ray tracing allows to compute both the phase and the amplitude of the ansatz (2), thus forming an approximate solution of (1). The phase ϕ can be simply computed as the integral of $\|P\|^2$ along a ray, since

$$\frac{d}{ds} \phi(Y(s)) = \frac{dY}{ds} \cdot \vec{\nabla} \phi(Y(s)) = \|P(s)\|^2 \quad (7)$$

Using (4), the amplitude a satisfies

$$\frac{d}{ds} a(Y(s)) = -a(Y(s)) \Delta \phi(Y(s)) - \nu a(Y(s)), \quad (8)$$

Of course, we need to specify initial conditions for (6)-(7)-(8), and this is where the notion of boundary conditions comes in.

Boundary conditions

Let us consider a bounded box containing our material. Outside this box, the vacuum is characterized by $N = 0$ (i.e. $n = 1$) and $\nu = 0$, and equation (1) simply reduces to the wave equation

$$\vec{\nabla}(\vec{\nabla} A) + k_0^2 A = 0$$

We assume that the incident component of A is a plane wave of direction unit vector \mathbf{e}_b

$$A_{inc}(X) = \exp(ik_0 X \cdot \mathbf{e}_b).$$

Let us denote Γ_{inc} the part of the boundary characterized by $\mathbf{e}_b \cdot \mathbf{w}_X < 0$, where \mathbf{w}_X is the outwards normal vector to the boundary of the domain at point X .

The comparison of the expression of the incident field A_{inc} with the W.K.B ansatz (2) provides initial conditions for (6)-(7)-(8). For all Y_0 on Γ_{inc} a ray entering the domain can be traced (one says shot) with the initial conditions

$$\begin{aligned} Y(0) &= Y_0 \\ P(0) &= \mathbf{e}_b \end{aligned}$$

(recall that P stands for the gradient of the phase). Equations (7)-(8) are solved with the initial conditions

$$\begin{aligned} \phi(Y(0)) &= Y_0 \cdot \mathbf{e}_b \\ a(Y(0)) &= 1. \end{aligned}$$

The phase gradient of the incident wave provides the initial condition for P , but also provides the initial value for ϕ simply by integrating it along Γ_{inc} . In this sense we say that we solve the Eikonal equation with the boundary condition on Γ_{inc}

$$\vec{\nabla} \phi = \mathbf{e}_b \tag{9}$$

In the following, the condition (9) will refer accordingly to the condition on the phase or to the condition on the gradient.

A solution ϕ of the Eikonal equation (3) and a solution a of the transport equation (4) are then computed along the rays flowing in the domain through Γ_{inc} with initial conditions given by A_{inc} . In this Lagrangian sense, $ae^{ik_0 \phi}$ is an approximation of a solution of (1).

In the presence of caustics, rays cross and yield multi-valued solutions a and ϕ at crossing points. Therefore the Lagrangian solution is a superposition of W.K.B. ansatz. We simplify further the problem in order to introduce a separation of the rays into an direct and a return part; we focus on the study of a single fold caustic. The notion of multi-valued solution of the Eikonal equation follows naturally.

An elementary example

In our setting the smooth variations of the index n are responsible for the scattering of the wave through the second equation of (6) which bends the rays. Let us assume that $X = (z, x) \in \mathbb{R} \times \mathbb{R}^+$, i.e. our domain is the half plane $x \geq 0$, and $\Gamma_{inc} = \{x = 0\}$. We take $\mathbf{e}_b = (\cos \alpha, \sin \alpha)$ with $\alpha \in]0, \frac{\pi}{2}[$ and select an index n which does not depends on z

$$N(x) = x ; n(x) = \sqrt{1 - x} \quad (10)$$

Let $Y_0 = (z_0, 0)$, $Y = (z, y)$ and $P = (q, p)$, The rays flowing through Γ_{inc} are a family of curves $(z(s, z_0), y(s, z_0))$ labeled by z_0 their initial position on $x = 0$ and parameterized by s . The ray equations (6) with the ad hoc initial conditions derived from (9) write

$$\begin{aligned} \frac{\partial z}{\partial s} &= q, \quad z(0) = z_0 \\ \frac{\partial y}{\partial s} &= p, \quad y(0) = 0 \\ \frac{\partial q}{\partial s} &= 0, \quad q(0) = \sin \alpha \\ \frac{\partial p}{\partial s} &= -\frac{1}{2}, \quad p(0) = \cos \alpha \end{aligned} \quad (11)$$

which defines a family of identical parabolic rays:

$$\begin{aligned} y(s, z_0) &= -\frac{1}{4}s^2 + s \cos \alpha \\ z(s, z_0) &= s \sin \alpha + z_0 \end{aligned} \quad (12)$$

Each ray therefore enters the domain with positive x -speed $\frac{\partial y}{\partial s} = \cos \alpha$; this speed decreases down to 0 which is reached at the point $x_c = \cos^2 \alpha$; afterwards the ray goes back with increasing negative x -speed $\frac{\partial y}{\partial s}$ until it exits the domain with $\frac{\partial y}{\partial s} = -\cos \alpha$ (see figure 2).

A first simplification which will be used throughout the paper is to use the z coordinate to parameterize the curve y . We remark indeed that z is a strictly increasing function of s and that we can reduce the dimensionality of the problem simply by writing y as a function of (z, z_0) :

$$y(z, z_0) = -\frac{1}{4} \left(\frac{z - z_0}{\sin \alpha} \right)^2 + \frac{z - z_0}{\sin \alpha} \cos \alpha \quad (13)$$

The domain spanned by the rays is bounded on one side by $\Gamma_{inc} = \{x = 0\}$ and on the other side by a curve $x = x_c = \cos^2 \alpha$ called caustic, which depends on the solution itself (here simply on the initial angle α). For $x > x_c$ the equation $x = y(z, z_0)$ has no real z_0 roots. This is the “shadow” region where no ray penetrates. When $x \leq x_c$ the equation $x = y(z, z_0)$ has two z_0 roots denoted z_0^- and z_0^+ which are functions of (z, x) . This is the illuminated region where every point (z, x) is reached by two rays:

- The first ray $y(\cdot, z_0^-)$ reaches (z, x) (i.e $x = y(z, z_0^-)$) before touching the caustic. This ray will be referred to as direct.

- The second ray $y(\cdot, z_0^+)$ reaches (z, x) (i.e $x = y(z, z_0^+)$) after touching the caustic. It will of course be our return ray.

We can also compute the phase by the ray method: equation (7) on the Lagrangian phase $\varphi(s, z_0)$ writes

$$\frac{\partial \varphi}{\partial s} = q^2 + p^2 = \frac{1}{4}s^2 - s \cos \alpha + 1 \quad (14)$$

We use again boundary condition (9): integrating it along Γ_{inc} yields $\varphi(0, z_0) = z_0 \sin \alpha$, assuming that $\varphi(0, 0) = 0$ since the solution of (3) is defined up to an additive constant. Therefore, solving (14) yields

$$\varphi(s, z_0) = \frac{1}{12}s^3 - \frac{1}{2}s^2 \cos \alpha + s + z_0 \sin \alpha$$

or if expressed as a function of (z, z_0) as in (13)

$$\varphi(z, z_0) = \frac{1}{12} \left(\frac{z - z_0}{\sin \alpha} \right)^3 - \frac{1}{2} \left(\frac{z - z_0}{\sin \alpha} \right)^2 \cos \alpha + \frac{z - z_0}{\sin \alpha} + z_0 \sin \alpha. \quad (15)$$

Coming back to our z_0^\pm splitting above we notice that the Lagrangian phase yields a bi-valued function of position (z, x) : $\varphi(z, z_0^\pm)$. If we want to shift to an Eulerian representation we therefore need two Eulerian phase functions $\phi^\pm(z, x)$ of (z, x) which are precisely defined by $\phi^\pm(z, x) = \varphi(z, z_0^\pm)$. Extracting the two roots of $x = y(z, z^\pm)$ we get

$$\phi^\pm(z, x) = \pm \frac{2}{3}(\cos^2 \alpha - x)^{3/2} + z \sin \alpha + \frac{2}{3} \cos^2 \alpha \quad (16)$$

We are now able to verify in this particular case the result in [8], which claims that the phases ϕ^\pm are the solutions of the PDE (3)

$$\frac{\partial \phi^{\pm 2}}{\partial z} + \frac{\partial \phi^{\pm 2}}{\partial x} = n^2(z, x)$$

with the same boundary condition imposed on ϕ^- on Γ_{inc} as in the ray method: $\phi^-(0, z) = z \sin \alpha$, and a boundary condition imposed on ϕ^+ at the caustic

$$\phi^+(z, x_c) = \phi^-(z, x_c) \quad (17)$$

relying on the fact that the Lagrangian phase $\phi(s, z_0)$ transported along the rays is continuous.

Recall that $P = (q, p)$ stands for the gradient of the phase. In our case $q = \sin \alpha$ is positive and constant in the whole domain, the Eikonal equation simplifies to

$$\frac{\partial \phi^\pm}{\partial x} = \mp \sqrt{n^2 - \sin^2 \alpha} \quad (18)$$

The choice of the \mp sign is the consequence of the \pm splitting convention: ϕ^- is the direct phase, the gradient of ϕ^- heads towards the caustic.

Integrating (18) with the boundary conditions described above we find again (16), thus proving that the resolution of the Eikonal equations on ϕ^\pm with boundary conditions (9) and (17) gives the same result as the ray method with boundary condition (9). Remark that we do not have to set a boundary condition on the caustic for the $-$ solution, nor on the incident boundary for the $+$ solution since the Eikonal equation is an hyperbolic equation, only the boundaries where the characteristics enter the domain are significant.

One goal of this paper is to achieve the same Eulerian splitting numerically when analytical solutions cannot be computed.

Motivations

We can now say a word about the motivations of this work. The main drawback of the ray method is that its spatial resolution depends on the field of rays, which is particularly dense near a caustic and sparse away from it. Therefore one needs sophisticated interpolation techniques as in [33] [46] to achieve a reasonable accuracy.

The original idea, also explored in [2] [7] [8] [15] [21] [38] [22] [40] [23] [25] [35] [42] [24] [30] [31] is to substitute an Eulerian method to ray tracing, which consists in solving the partial differential equation (3) on a fixed grid instead of computing the phase along rays. This allows an arbitrary uniform spatial resolution depending only on the mesh. The difficulty is to take into account the possible multivaluedness of the ray field.

This paper presents an Eulerian numerical method for the computation of a bi-valued solution in a geometric setting similar to our simplified toy problem above. More precisely we will consider $+$ and $-$ solutions connected in the Eulerian sense (17) along a caustic curve which can be parameterized by z . Such caustics are called folds (the ray field folds on itself).

In most applications concerning the absorption of a laser in a plasma, there exists a privileged ray propagation direction denoted z such that, setting $X = (z, x) \in \mathbb{R} \times \mathbb{R}^d$, equation (3) may be written as

$$\frac{\partial \phi}{\partial z} + H(z, x, \frac{\partial \phi}{\partial x}) = 0 \quad (19)$$

where in our case

$$H(z, x, p) = -\sqrt{n^2(z, x) - p^2} \quad (20)$$

Our work applies to the general abstract framework of Hamilton-Jacobi equations, where the Hamiltonian H is continuous up to its second derivatives and strictly convex in its last variable.

Organization of the paper

We first recall (section 1) some mathematical properties of fold solutions of the equation (19) in its Lagrangian and Eulerian settings. We then derive, in section 2, an ODE for the equation of a general caustic curve of the form $x = x_c(z)$, which closes the Eulerian system for the $-$ and $+$ solution. In practice, the initialization is only given for the $-$ part of the solution; we explain how to construct a bi-valued stationary solution that can be used as an initialization of the complete \pm system in the general case. The difficulties linked with the discretization of the Eulerian system are discussed in section 3 where we propose an approximate numerical closure for the caustic equation. Section 4 presents some numerical results.

A sequel to this paper [11] is devoted to the computation of the energy (5).

1 Mathematical tools

We consider the Hamiltonian function (20)

$$H(z, x, p) = -\sqrt{n^2(z, x) - p^2}$$

We assume that the index n and the direct condition are such that the multi-valued solution of the Hamilton-Jacobi equation (19) exhibits a fold caustic. Let us introduce these notions in the framework of bicharacteristics.

1.1 The bicharacteristics

We consider the following set of ordinary differential equations, called the Hamiltonian system

$$\begin{cases} \dot{y}(z, x_0) = H_p(z, y, p) \\ \dot{p}(z, x_0) = -H_x(z, y, p) \\ \dot{\varphi}(z, x_0) = p \cdot H_p(z, y, p) - H(z, y, p) \end{cases} \quad (21)$$

with initial conditions

$$\begin{cases} y(0, x_0) = x_0 \\ p(0, x_0) = \partial_{x_0} \phi_0(x_0) \\ \varphi(0, x_0) = \phi_0(x_0) \end{cases}$$

The dot stands for derivation with respect to z , and H_x and H_p denote the derivatives of H with respect to x and p .

The curves $(z, x_0) \mapsto (y(z, x_0), p(z, x_0))$ are called the bicharacteristics. The rays $(z, x_0) \mapsto y(z, x_0)$ are the projection onto the first coordinate of the bicharacteristics. To each initial position $x_0 \in \mathbb{R}^d$ corresponds a ray $z \mapsto y(z, x_0)$ parameterized by z .

The phase $\varphi(z, x_0)$ is computed along the corresponding ray $y(z, x_0)$, i.e. the value of the phase at point $(z, y(z, x_0))$ is $\varphi(z, x_0)$. When rays cross, φ is multi-valued. This happens in particular in the vicinity of a caustic.

1.2 The caustic

Definition 1.1. *The caustic is the set of the points $(z, y(z, x_0))$ such that*

$$\partial_{x_0} y(z, x_0) = 0 \quad (22)$$

Proposition 1.1. *The caustic is the envelope of the rays*

Proof. The envelope of a family of curves $(z, y(z, x_0))$ depending on two parameters z and x_0 is the set of the points $(z, y(z, x_0))$ such that the Jacobian of the map $(z, x_0) \mapsto (z, y(z, x_0))$ vanishes. \square

The Lagrangian method for computing the position of the caustic is to compute $\partial_{x_0}y$ along the rays. Indeed, linearizing the hamiltonian system with respect to x_0 yields a set of ordinary differential equations [8]

$$\partial_z \begin{pmatrix} \partial_{x_0}y \\ \partial_{x_0}p \end{pmatrix} = \begin{pmatrix} H_{xp}(z, y, p) & H_{pp}(z, y, p) \\ -H_{xx}(z, y, p) & -H_{xp}(z, y, p) \end{pmatrix} \begin{pmatrix} \partial_{x_0}y \\ \partial_{x_0}p \end{pmatrix} \quad (23)$$

the initial condition being

$$\begin{pmatrix} \partial_{x_0}y(0, x_0) \\ \partial_{x_0}p(0, x_0) \end{pmatrix} = \begin{pmatrix} 1 \\ \partial_{x_0}^2 \phi_0 \end{pmatrix}$$

Since the initial condition is non zero, we have the following result:

Lemma 1.1. *$\partial_{x_0}y$ and $\partial_{x_0}p$ cannot vanish simultaneously.*

Regularity conditions

Until now we have been implicitly working in a \mathcal{C}^∞ framework. For the need of section 2.2, we give here minimal regularity conditions on n and ϕ_0 to achieve the continuity of the caustic.

Lemma 1.2. *We assume that:*

- $n(z, x)$ is continuous with respect to z and \mathcal{C}^3 with respect to x ;
- $\phi_0(x_0)$ is \mathcal{C}^3 .

Then $y(z, x_0)$ and $\partial_{x_0}y(z, x_0)$ are \mathcal{C}^1 functions.

Proof. See for instance theorem 3.4.2 p.148 in [17] on the regularity of the solution of an ODE with respect to the initial condition. \square

Proposition 1.2. *Under the above assumptions, the caustic is a continuous curve.*

Proof. The caustic can be parametrized by x_0 . Indeed,

$$\partial_z(\partial_{x_0}y) = H_{xp}(z, y, p)\partial_{x_0}y + H_{pp}(z, y, p)\partial_{x_0}p$$

At a caustic point, $\partial_{x_0}y$ vanishes, but $\partial_{x_0}p$ does not (lemma1.1). Moreover, $H_{pp} > 0$ due to the strict convexity of H with respect to p . Therefore in the vicinity of a caustic point, $\partial_{zx_0}^2 y \neq 0$. Therefore we can apply the implicit function theorem: there exists a \mathcal{C}^1 function $z(x_0)$ such that

$$\partial_{x_0}y(z(x_0), x_0) = 0$$

Then the caustic is the curve $\{(z(x_0), y(z(x_0), x_0))\}$. \square

The fold caustic

In dimension 2 there are two kinds of stable caustics, the fold caustic and the cuspidal caustic [5] [29]. As mentioned in the introduction, we focus on fold caustics.

Definition 1.2. *The caustic point $(z, y(z, x_0))$ is a fold caustic point if and only if*

$$\partial_{x_0}^2 y(z, x_0) \neq 0 \quad (24)$$

Proposition 1.3. *The fold caustic is a curve that can be parameterized by z . We denote it $x = x_c(z)$.*

Proof. Since $\partial_{x_0}^2 y(z, x_0) \neq 0$, one can apply the implicit function theorem: there exists a function $x_0(z)$ such that $\forall z, \partial_{x_0} y(z, x_0(z)) = 0$. Then the caustic is the curve $x = y(z, x_0(z))$. \square

1.3 Switching to an Eulerian framework

The variables (z, x_0) are called ray or Lagrangian coordinates. The variables (z, x) are called Eulerian coordinates. We call Lagrangian (resp. Eulerian) a function of the Lagrangian (resp. Eulerian) coordinates.

When the transformation from Lagrangian to Eulerian coordinates

$$(z, x_0) \mapsto (z, y(z, x_0)) \quad (25)$$

is invertible, that is out of caustic points according to definition 1.1, the Lagrangian phase $\varphi(z, x_0)$ defines locally an Eulerian function $\phi(z, x)$ by

$$\phi(z, y(z, x_0)) = \varphi(z, x_0) \quad (26)$$

(see figure 1).

A theorem in [27] states that the second coordinate p of the bicharacteristics (shot with the proper initial conditions) matches the gradient of the Eulerian phase:

$$p(z, x_0) = \partial_x \phi(z, y(z, x_0)) \quad (27)$$

Assuming this, we prove

Proposition 1.4. *The function ϕ is solution of the Hamilton-Jacobi equation*

$$\partial_z \phi(z, x) + H(z, x, \partial_x \phi(z, x)) = 0 \quad (28)$$

Proof. Deriving definition (26) with respect to z yields

$$\partial_z \phi + \dot{y} \cdot \partial_x \phi = \dot{\varphi} = p \cdot H_p(z, y, p) - H(z, y, p)$$

which simplifies using (21): $\dot{y} = H_p$ and (27): $p = \partial_x \phi$. \square

One can therefore compute the phase in an Eulerian framework by solving the partial differential equation (28) on a fixed grid, thus avoiding the resolution problems of the ray method. However, this is not straightforward, because of multivaluedness and caustics. This paper presents an Eulerian method for computing the phase in the vicinity of a fold caustic.

1.4 Behavior of the phase in the vicinity of a fold caustic

We provide here some material for later use. In order to describe the behavior of the phase, we study a geometrical object which is the graph of the gradient of the phase (or rather p) in a generalized meaning since the phase is multivalued. Let us consider the manifold consisting of the union of all bicharacteristics,

$$\Lambda = \{(z, y(z, x_0), p(z, x_0)) \mid z \geq 0, x_0 \leq 0\} \quad (29)$$

Remark: Λ is the projection of what is usually called the Lagrangian manifold [20]. We do not take into account the dual coordinate of z since z is a privileged direction of propagation and no folding can occur in this direction.

Proposition 1.5. Λ is a manifold of dimension 2

Proof. The Jacobian matrix of the map defining Λ in (29) is

$$\begin{pmatrix} 1 & \partial_z y & \partial_z p \\ 0 & \partial_{x_0} y & \partial_{x_0} p \end{pmatrix}$$

Since $\partial_{x_0} y$ and $\partial_{x_0} p$ do not vanish simultaneously (lemma 1.1), there is always one of the two matrices

$$\begin{pmatrix} 1 & \partial_z y \\ 0 & \partial_{x_0} y \end{pmatrix} \text{ and } \begin{pmatrix} 1 & \partial_z p \\ 0 & \partial_{x_0} p \end{pmatrix}$$

which is invertible. □

This proof points out that the caustic, where $\partial_{x_0} y$ vanishes, is the set of points above which Λ cannot be parameterized by z and x . This means that Λ has a vertical tangent plane, and is no longer a graph. However, at caustic points $\partial_{x_0} p$ does not vanish and Λ can be parameterized by z and p . In the case of the fold caustic, Λ remains on one side of the tangent plane (which is not the case at the tip of a cuspidal caustic), as shown by corollary 1.1.

Let (z_c, x_c) be a caustic point. Let x_0 be the initial position of the ray that hits (z_c, x_c) , i.e. $x_c = y(z_c, x_0)$. Let p_c denote the corresponding value of p , $p(z_c, x_0)$. Since $\partial_{x_0} p(z_c, x_0) \neq 0$, Λ can be parameterized by z and p in the vicinity of (z_c, x_c, p_c) . Let $x(z, p)$ be the function such that

$$\Lambda = \{(z, x(z, p), p)\}$$

Lemma 1.3. $\partial_p x(z_c, p_c) = 0$ and $\partial_{p^2}^2 x(z_c, p_c) \neq 0$

Proof. By definition (29), function $x(z, p)$ satisfies

$$x(z, p(z, x_0)) = y(z, x_0)$$

Deriving with respect to x_0 yields

$$\begin{aligned}\partial_{x_0} p \partial_p x &= \partial_{x_0} y \\ \partial_{x_0}^2 p \partial_p x + (\partial_{x_0} p)^2 \partial_p^2 x &= \partial_{x_0}^2 y\end{aligned}$$

which proves the lemma using the fact that at a fold caustic point $\partial_{x_0} y = 0$, $\partial_{x_0}^2 y \neq 0$ and $\partial_{x_0} p \neq 0$ \square

Corollary 1.1. *The Taylor expansion of $x(z, p)$ with respect to p is*

$$x(z_c, p) = x_c + a(z_c)(p - p_c)^2 + O((p - p_c)^3) \quad (30)$$

where $a(z_c) = \partial_{p^2}^2 x(z_c, p_c)$ does not vanish.

2 Derivation of the complete model

We consider a setting in which the Lagrangian phase φ exhibits a fold caustic. It then defines two Eulerian functions ϕ^\pm that are related at the caustic by the continuity condition (17) and are solutions (see [8]) of the Hamilton-Jacobi equations

$$\begin{cases} \partial_z \phi^- + H(z, x, \partial_x \phi^-) = 0 \\ \partial_z \phi^+ + H(z, x, \partial_x \phi^+) = 0 \end{cases} \quad (31)$$

in the illuminated region bounded by the caustic curve \mathcal{C} with a boundary condition derived from (17)

$$\phi^+|_{\mathcal{C}} = \phi^-|_{\mathcal{C}}.$$

According to proposition 1.3, this curve can be parameterized by z in the form $x = x_c(z)$ and we derive below an ODE for x_c (see section 2.1). Let us assume for simplicity that the computational domain (the illuminated region) lies on the left of the caustic ($x \leq x_c(z)$). For obvious technical reasons, we have to bound our domain on the left. We assumed that the index of refraction was constant (free space) for $x \leq 0$. In this region of free propagation, the physics relies on the unit vector $e_b = (\sin \alpha, \cos \alpha)$ describing the direction of the incident laser beam. We therefore restrain the computational domain to $0 \leq x \leq x_c(z)$. As explained in the introduction, the boundary condition on $x = 0$ (also called Γ_{inc}) for the $-$ part of the solution depends on e_b and is given by (assume that $\phi^-(0, 0) = 0$ and $n(z, x) = 1$ for $x \leq 0$):

$$\phi^-(z, 0) = \phi_{inc}(z) = z \sin \alpha.$$

We enforce an outgoing boundary condition for ϕ^+ on $x = 0$ under the geometrical fold hypothesis that the return rays exit the domain once they have turned at the caustic. This can be easily implemented using Sonner's type boundary conditions (see [6] [1])

$$\phi^+(z, 0) = +\infty.$$

The geometrical setting of the problem is further complicated as the ideal half plane situation of the introduction with a pseudo-stationary in z fold solution is of course not the general rule. In practice the index of refraction modelizing the plasma is given in a bounded box $0 \leq x \leq x_d$, $0 \leq z \leq z_d$ where z_d is our final z horizon and x_d necessarily satisfies $x_d > x_c(z)$ for all z . Then the actual domain of definition of ϕ^- and ϕ^+ depends on the geometry of the extremal ray shot from the $(0,0)$ corner (see figure 3). We show in section 2.2 how to extend the domains of definition of ϕ^- and ϕ^+ in a non interfering way by imposing compatible initial conditions ϕ_0^- and ϕ_0^+ on ϕ^- and ϕ^+ . The caustic is also virtually prolonged and starts at $z = 0$. We denote $C_0 = x_c(0)$.

2.1 Equation of the caustic

As noted in [8] the problem is a free boundary problem since the domain is bounded by the caustic, which itself depends on the solution. The position of the caustic is therefore an unknown of the problem. We derive here a new equation for this unknown. It is one of the key ingredients in the closure of our system.

Let $x_0(z)$ be the function such that for all $z \geq 0$, $x_0(z)$ is the starting point of the ray that hits the caustic at time z , which writes $x_c(z) = y(z, x_0(z))$. Deriving with respect to z yields

$$\dot{x}_c(z) = \dot{y} + \partial_z x_0 \cdot \partial_{x_0} y$$

At caustic points, $\partial_{x_0} y = 0$. Therefore, using (21),

$$\dot{x}_c(z) = H_p(z, x_c(z), p_c(z)) \quad (32)$$

where $p_c(z) = p(z, x_0(z))$ is the value of p at the caustic.

In order to compute the position of the caustic $x_c(z)$ through an ordinary differential equation, we would need to compute $p_c(z)$ as well. Deriving $p_c(z) = p(z, x_0(z))$ with respect to z yields

$$\dot{p}_c(z) = \dot{p} + \partial_z x_0 \cdot \partial_{x_0} p$$

There appears $\partial_z x_0$ which is unknown, and $\partial_{x_0} p$ which does not vanish. Therefore we cannot compute an ODE on $x_c(z)$ independently. It is necessary to couple it to the resolution of the Eikonal equations (31); indeed, relation (27) shows that $p_c(z) = \partial_x \phi^-(z, x_c(z)) = \partial_x \phi^+(z, x_c(z))$, and we should be able to recover p_c from ϕ^- and ϕ^+ . However, numerical difficulties linked to the behavior of the phase in the vicinity of the caustic must be addressed (see section 3.1).

2.2 Initial conditions

In this section we propose a systematic way of deriving a non interfering Cauchy data for our system (31)-(32). The idea is to consider a stationary problem similar to the toy problem of the introduction in the $z \leq 0$ zone.

We first extend the refraction index n by setting

$$n(z, x) = n(0, x) \text{ for } z < 0$$

Note that the index thus defined complies with the regularity condition of proposition 1.2.

We then set a “stationary” direct condition on $\mathbb{R}^- \times \{0\}$ which, assuming again that $n(z, 0) = 1$ and $\phi^-(0, 0) = 0$, takes the form

$$\phi^-(z, 0) = \phi_{inc}(z) = z \sin \alpha.$$

This just means that all rays shot from $\mathbb{R}^- \times \{0\}$ are shot with the same angle α .

We now give a sufficient condition for the existence of a caustic: let us assume that there exists a point x such that $n(0, x) = \sin \alpha$ and that the infimum C_0 of such points is such that $\partial_x n(0, C_0) < 0$, which will be the case in our application.

Proposition 2.1. *Under these assumptions, the Lagrangian solution φ exhibits a fold caustic in the $z < 0$ region. This caustic is the vertical line $x = C_0$.*

Proof. The rays solve an equation analogous to (11),

$$\begin{aligned} \partial_s y &= p \\ \partial_s p &= \partial_x(n^2(0, y)) \end{aligned}$$

Substituting the first equation in the second one, multiplying by $\partial_s y$ and integrating yields $(\partial_s y)^2 = n^2(0, y) - \sin^2 \alpha$, or

$$\partial_s y = \pm \sqrt{n^2(0, y) - \sin^2 \alpha}$$

Each ray therefore enters the domain with positive x -speed and propagates to the right until it reaches C_0 where $\partial_s y$ vanishes. There the condition $\partial_x n(0, C_0) < 0$ ensures that $\partial_s y$ changes signs and that the ray propagates to the left until it exits the domain.

This qualitative study proves that the Lagrangian solution φ of the Hamiltonian system (21) with the above prescribed incident wave condition exhibits a fold caustic at $x = C_0$. \square

We denote by ϕ^\pm the corresponding Eulerian functions, defined for $z \leq 0$ and $0 \leq x \leq C_0$. The value at $z = 0$ of these phases will of course be our initial conditions for ϕ^\pm in (36): we now consider our problem (36) for $z > 0$ as the continuation of a stationary case, in which we compute everything explicitly (see below). Note that it extends the caustic, supposedly starting at some $z_0 > 0$, when the extremal ray (starting from $(0, 0)$) first hits the caustic, with a “virtual” caustic, vertical in negative z (see figure 4). The virtual caustic smoothly rejoins the caustic we want to compute at $z = z_0$. This conjecture is theoretically justified by proposition 1.2 and numerically confirmed by the results of section 4.

Explicit computation of the initial conditions

As shown by the bicharacteristics method, $\partial_z \phi^\pm$ is constant and equal to $\sin \alpha$ in the whole $z \leq 0$ domain since $\frac{\partial q}{\partial s} = 0$ in (11). Therefore we can set

$$\phi^\pm(z, x) = \phi_0^\pm(x) + z \sin \alpha$$

and from the Eikonal equation (19) we deduce that ϕ_0^- and ϕ_0^+ solve

$$\frac{\partial \phi_0^\pm}{\partial x} = \mp \sqrt{n^2 - \sin^2 \alpha} \quad (33)$$

(since ϕ^- corresponds to the direct part of the rays, its gradient must head to the right). The functions ϕ_0^\pm can be computed by integration:

$$\begin{aligned} \phi_0^-(x_0) &= \int_0^{x_0} \sqrt{n^2(0, x) - \sin^2 \alpha} \, dx \\ \phi_0^+(x_0) &= \phi_0^-(C_0) + \int_{x_0}^{C_0} \sqrt{n^2(0, x) - \sin^2 \alpha} \, dx \end{aligned}$$

assuming that $\phi_0^-(0) = 0$ and using boundary condition (17).

2.3 Change of variables

For mere practical purposes, we make a change of variables that will simplify the geometry of our computational domain, and make its discretization easier. Let

$$\tilde{x}(z, x) = x - x_c(z) + C_0 \quad (34)$$

In the new variable \tilde{x} , the equation of the caustic writes

$$\tilde{x} = C_0$$

The caustic is then a straight line, and the computational domain is simply $\mathbb{R}^+ \times [0, C_0]$.

Let us now determine the equation satisfied by ϕ after this change of variables. Let $\tilde{\phi}(z, \tilde{x}) = \phi(z, x)$. The Eikonal equation becomes

$$\partial_z \tilde{\phi} - \dot{x}_c(z) \partial_{\tilde{x}} \tilde{\phi} + H(z, \tilde{x} + x_c(z) - C_0, \partial_{\tilde{x}} \tilde{\phi}) = 0 \quad (35)$$

or

$$\partial_z \tilde{\phi} + \tilde{H}(z, \tilde{x}, \partial_{\tilde{x}} \tilde{\phi}) = 0$$

where

$$\tilde{H}(z, \tilde{x}, p) = H(z, \tilde{x} + x_c(z) - C_0, p) - \dot{x}_c(z)p$$

We remark that the modified Hamiltonian \tilde{H} remains convex in its last variable p .

2.4 Summary

For convenience we summarize here all the equations and boundary/initial conditions

Equation (32) on $x_c(z)$ is added to system (31). After change of variables (34), we get the following system of equations

$$\begin{cases} \partial_z \tilde{\phi}^- + \tilde{H}(z, \tilde{x}, \partial_{\tilde{x}} \tilde{\phi}^-) = 0 \\ \partial_z \tilde{\phi}^+ + \tilde{H}(z, \tilde{x}, \partial_{\tilde{x}} \tilde{\phi}^+) = 0 \\ \dot{x}_c(z) = H_p(z, x_c(z), p_c(z)) \\ p_c(z) = \partial_{\tilde{x}} \tilde{\phi}^\pm(z, C_0) \end{cases} \quad \text{for } (z, x) \in \mathbb{R}^+ \times [0, C_0] \quad (36)$$

Remark: the Eikonal equations are coupled to the additional ordinary differential equation on $x_c(z)$ since \tilde{H} depends on x_c .

We impose the following boundary conditions:

- Incident wave boundary condition:

$$\tilde{\phi}^-(z, 0) = \phi_{inc}(z) \text{ for } z \geq 0$$

- Condition on the caustic:

$$\tilde{\phi}^+(z, C_0) = \tilde{\phi}^-(z, C_0) \text{ for } z \geq 0$$

- Outgoing boudary conditions:

We impose a Soner's type outgoing condition on $\tilde{\phi}^+$ on Γ_{inc} , and on $\tilde{\phi}^-$ on the caustic.

- Initial conditions:

$$\begin{aligned} \tilde{\phi}^\pm(0, x_0) &= \phi_0^\pm(x_0) \\ x_c(0) &= C_0 \end{aligned}$$

3 Numerical methods

In order to solve the Eikonal equations in (36), we use a finite differences scheme based upon the Osher-Godunov numerical Hamiltonian. We write it down in section 3.3 only because our Hamiltonian is not the classical Hamiltonian of geometric optics.

The originality of our method consists in solving simultaneously the ordinary differential equation (32) on the position of the caustic, which is one of the boundaries of our computational domain. The main difficulty here is to compute an accurate value of p_c (see section 3.1). We also clarify the boundary condition used on the caustic in section 3.2.

Notations

Let $\{\tilde{x}_1, \dots, \tilde{x}_J\}$ be the regular discretization of $[0, C_0]$. The z discretization $\{z^n\}$ follows by application of a CFL type condition, depending on the angle of the rays with the x -axis (the smaller this angle, the stricter the CFL condition). Let δz and δx be the steps of discretization.

The value of a function a at point (z^n, \tilde{x}_j) is denoted a_j^n , and $\partial_{\tilde{x}}^l a_j^n$ and $\partial_{\tilde{x}}^r a_j^n$ stand for its numerical discrete left and right derivatives. Let us start with a finite differences scheme of order 1. Upwind derivative operators are:

$$\begin{aligned}\partial_{\tilde{x}}^l a_j^n &= \frac{a_j^n - a_{j-1}^n}{\delta x} \\ \partial_{\tilde{x}}^r a_j^n &= \frac{a_{j+1}^n - a_j^n}{\delta x}\end{aligned}$$

3.1 Computation of p_c

The resolution of (32) requires an accurate computation p_c , which is the limit value of the gradient of both phases ϕ^\pm at the caustic.

Remark

Under the change of variables (34),

$$\partial_{\tilde{x}} \tilde{\phi} = \partial_x \phi$$

Therefore it suffices to study the relationship between p_c and the gradients of the phases in the old variable x . Moreover, we fix z in all this section, and often omit dependence on z .

Difficulties encountered

Thanks to relation (27), we know that $p_c(z) = \partial_x \phi^-(z, x_c(z)) = \partial_x \phi^+(z, x_c(z))$. However, the discrete estimations of the gradient of the phase with respect to x using finite differences in the vicinity of the caustic are inaccurate because of the generic behavior of the phase in the vicinity of the caustic. Let us sketch the convergence of the finite differences scheme. We omit dependence on z and denote by ϕ' , ϕ'' and ϕ''' the first derivatives of ϕ with respect to x . The Taylor formula writes

$$\phi'(x) = \frac{\phi(x) - \phi(x - \delta x)}{\delta x} - \frac{\delta x}{2} \phi''(x) + o(\delta x)$$

Formally, $\phi''(x) \sim \frac{1}{\sqrt{x_c - x}}$ and letting $x \rightarrow x_c$ in Taylor's formula yields

$$\phi'(x_c) - \frac{\phi(x_c) - \phi(x_c - \delta x)}{\delta x} \sim \sqrt{\delta x}$$

The estimation of p_c with the discrete derivative of ϕ^- or ϕ^+ would therefore only be of order $\frac{1}{2}$, and pollute our scheme, otherwise of order 1.

Worse, increasing the order of the finite differences scheme does not improve things at all. Of course,

$$\phi'(x) = \frac{3\phi(x) - 4\phi(x - \delta x) + \phi(x - \delta x)}{2\delta x} + \frac{2}{3}\phi'''(x)\delta x^2 + o(\delta x^2)$$

but $\phi'''(x) \sim \frac{1}{(x_c - x)^{3/2}}$, hence

$$\phi'(x_c) - \frac{3\phi(x_c) - 4\phi(x_c - \delta x) + \phi(x_c - \delta x)}{2\delta x} \sim \sqrt{\delta x}$$

But, as we shall see, the approximate numerical values of order $\frac{1}{2}$ of $\partial_x \phi^\pm$ in the vicinity of the caustic will still allow us to get an approximation of p_c of order 1, thanks to the knowledge of the geometry of manifold Λ in the vicinity of a fold caustic.

Heuristics

This paragraph mathematically illustrates formula (37). As shown on figure 6, the direction of the caustic is approximated by the mean value of the directions of the rays at some point close to the caustic. The key ingredient here is that the errors, of order $\frac{1}{2}$, made in the computation of the gradients of the phases are suppressed, thanks to the local symmetry of manifold Λ , the order of the error being thus improved from $\frac{1}{2}$ to 1.

More precisely, let us consider a cut of Λ at z fixed, as on figure 5. Let p^- and p^+ denote the direct and return values of p at point $x_c - \delta x$, i.e.

$$p^\pm = \partial_x \phi^\pm(z, x_c - \delta x)$$

Corollary 1.1 shows that Λ is locally an approximate parabola of vertex (x_c, p_c) . If it were an exact parabola, we would have $p_c = \frac{p^+ + p^-}{2}$. In the general case, we have, as $\delta x \rightarrow 0$,

$$\frac{p^+ + p^-}{2} = p_c + O(\delta x)$$

Proof. Since $p^+ \rightarrow p_c$ and $p^- \rightarrow p_c$, one can apply Taylor approximation (30) of x as a function of p :

$$x_c - \delta x = x(p^\pm) = x_c + A(p^\pm - p_c)^2 + O((p^\pm - p_c)^3)$$

where A does not vanish. First, we deduce an estimate of $p^\pm - p_c$:

$$A(p^\pm - p_c)^2 \sim -\delta x \Rightarrow p^\pm - p_c \sim \pm B\sqrt{\delta x}$$

where $B = \frac{-1}{\sqrt{|A|}}$ ($p^- > p_c$ is the direction of the direct rays). Then,

$$\begin{aligned} A(p^\pm - p_c)^2 &= -\delta x + O((p^\pm - p_c)^3) = -\delta x + O(\delta x^{\frac{3}{2}}) \\ \Rightarrow p^\pm - p_c &= \pm B\sqrt{\delta x} + O(\delta x) \end{aligned}$$

Summing the \pm equalities yields

$$\frac{p^+ + p^-}{2} - p_c = O(\delta x)$$

□

Thanks to the symmetry up to $O((p - p_c)^3)$ of manifold Λ , the $\sqrt{\delta x}$ terms simplify, having the same coefficient.

Numerical estimate for p_c

In practice, we work with a discretization of ϕ^\pm , and discrete derivatives. Let

$$\tilde{p}^\pm = \frac{\phi^\pm(x_c) - \phi^\pm(x_c - \delta x)}{\delta x}$$

be the discrete derivatives of ϕ^\pm , centered at $x_c - \delta x/2$. Then a numerical estimate for p_c is

$$\tilde{p}_c = \frac{\tilde{p}^+ + \tilde{p}^-}{2} \tag{37}$$

Proposition 3.1. *As $\delta x \rightarrow 0$, $\tilde{p}_c = p_c + O(\delta x)$.*

Proof. As in the previous proof, (30) yields

$$p^\pm(x) = p_c \pm B\sqrt{x_c - x} + O(x_c - x)$$

which leads by integration to

$$\phi^\pm(x) = \phi^\pm(x_c) + p_c(x - x_c) \mp \frac{2}{3}B(x_c - x)^{3/2} + O((x_c - x)^2)$$

Hence

$$\tilde{p}^\pm = \frac{\phi^\pm(x_c) - \phi^\pm(x_c - \delta x)}{\delta x} = p_c \pm \frac{2}{3}B\sqrt{\delta x} + O(\delta x)$$

and, summing the \pm equalities,

$$\tilde{p}_c = p_c + O(\delta x)$$

□

Remark: the penultimate relation proves what had been only sketched, that finite differences applied to ϕ^- or ϕ^+ only give an approximation \tilde{p}^\pm of p_c of order $\frac{1}{2}$.

Upwinding

Eventually, one has to take into account that the values of the phase used to compute p_c in our algorithm are numerical values computed at previous step, and not exact values as above. The pseudo-stationary case (the index n does not depend on z) gives an indication that an upwind formulae may be better than centered derivatives for the computation of \tilde{p}^\pm . Indeed, in that case $\partial_z \phi^\pm$ is constant and the caustic is a vertical line i.e. $p_c = 0$. The direction of the upwinding for ϕ^\pm is known and the semi-discretization of the Eikonal equations gives

$$\begin{aligned}\partial_z \phi^- + \sqrt{n^2(x_j) - \left(\frac{\phi_j^- - \phi_{j-1}^-}{\delta x}\right)^2} &= 0 \\ \partial_z \phi^+ + \sqrt{n^2(x_j) - \left(\frac{\phi_{j+1}^+ - \phi_j^+}{\delta x}\right)^2} &= 0\end{aligned}$$

and denoting $c = \partial_z \phi^\pm$, the numerical solution satisfies

$$\begin{aligned}\frac{\phi_j^- - \phi_{j-1}^-}{\delta x} &= \sqrt{n^2(x_j) - c^2} \\ \frac{\phi_{j+1}^+ - \phi_j^+}{\delta x} &= -\sqrt{n^2(x_j) - c^2}\end{aligned}$$

. Using upwind derivatives to compute \tilde{p}^\pm yield and exact $p_c = 0$ in formula (37).

3.2 Boundary condition at the caustic

The boundary condition at the caustic for ϕ^+ is the value of the phase at the caustic, given by the former computation of ϕ^- . We stress here that the value yielded by the Osher-Godunov Hamiltonian based scheme is inaccurate, and that it is possible and preferable to compute this value by solving an additional ordinary differential equation.

Let $\phi_c(z) = \varphi(z, x_0(z))$ be the value of the phase at the caustic. Numerically, we will rather take $\phi^+(z, x_c(z)) = \phi_c(z)$ than $\phi^+(z, x_c(z)) = \phi^-(z, x_c(z))$ as a boundary condition. Indeed, as shown below, the computation of the ordinary differential equation on ϕ_c (39) using our numerical estimate for p_c is more accurate than the computation of the Eikonal equation on $\tilde{\phi}^-$ in the last mesh at the caustic (38) using the numerical Hamiltonian.

More precisely, the modified Eikonal equation (35) at caustic point $\tilde{x} = C_0$ writes

$$\partial_z \tilde{\phi}^-(z, C_0) = \partial_{\tilde{x}} \tilde{\phi}^- \cdot H_p(z, x_c(z), p_c(z)) - H(z, x_c(z), \partial_{\tilde{x}} \tilde{\phi}^-)$$

and the numerical scheme in last mesh J yields

$$\partial_z \tilde{\phi}_J^- = \partial_{\tilde{x}}^l \tilde{\phi}_J^- \cdot H_p(z, x_c, \tilde{p}_c) - H(z, x_c, \partial_{\tilde{x}}^l \tilde{\phi}_J^-) \quad (38)$$

(here we only discretize in space).

Besides, $\dot{\phi}_c(z) = \dot{\phi}(z, x_0(z)) + \partial_z x_0 \partial_{x_0} \varphi(z, x_0(z))$, therefore using the third line of the Hamiltonian system (21) and $\partial_{x_0} \varphi(z, x_0(z)) = 0$, we get

$$\dot{\phi}_c(z) = p_c(z) H_p(z, x_c(z), p_c(z)) - H(z, x_c(z), p_c(z))$$

The corresponding numerical scheme is

$$\dot{\phi}_c = \tilde{p}_c H_p(z, x_c, \tilde{p}_c) - H(z, x_c, \tilde{p}_c) \quad (39)$$

Comparing both schemes (38) and (39) shows that in the second one, $\partial_{\tilde{x}} \tilde{\phi}^-$ has been replaced by \tilde{p}_c . We saw in section 3.1 that \tilde{p}_c is an approximation of p_c of order 1 (proposition 3.1), whereas $\partial_{\tilde{x}} \tilde{\phi}^-$ is only an approximation of order $\frac{1}{2}$.

And indeed, numerical simulations show that the estimation of ϕ_c through (38) is of order $\frac{1}{2}$ only, whereas using (39) we get an estimation of order 1.

3.3 The numerical Hamiltonian

We give an almost closed formula for the sake of completeness. Let u^l and u^r be the left and right discrete derivatives of $\tilde{\phi}$. Osher-Godunov's numerical Hamiltonian [37] \hat{H} is given by

$$\hat{H}(z, \tilde{x}, u^l, u^r) = \text{ext}_{u \in [u^l, u^r]} \tilde{H}(z, \tilde{x}, u)$$

where

$$\text{ext}_{u \in [a, b]} = \begin{cases} \min_{a \leq u \leq b} & \text{if } a \leq b \\ \max_{b \leq u \leq a} & \text{if } a > b \end{cases}$$

The numerical Hamiltonian does not simplify to a modmax as usual because of the additional linear term in p , due to change of variables (34). However, notice that function $p \mapsto -\sqrt{n^2 - p^2} - \dot{x}_c p$ reaches minimum at point $n\dot{x}_c / \sqrt{1 + \dot{x}_c^2}$. Therefore,

$$\hat{H}(z, \tilde{x}, u^l, u^r) = \tilde{H}(z, \tilde{x}, \hat{u})$$

where

$$\hat{u} = \text{modmax} \left(\max(u^l - \frac{n\dot{x}_c}{\sqrt{1 + \dot{x}_c^2}}, 0), \min(u^r - \frac{n\dot{x}_c}{\sqrt{1 + \dot{x}_c^2}}, 0) \right) + \frac{n\dot{x}_c}{\sqrt{1 + \dot{x}_c^2}}$$

except when $u^r < n\dot{x}_c / \sqrt{1 + \dot{x}_c^2} < u^l$, where one has to come back to the initial formula and test which out of the two derivatives yields maximal value of function \tilde{H} (ext being max in that case).

3.4 The algorithm

We write down here in full extent how the numerical methods we propose are implemented. Given the values at time z^n at all points $j \in \{1 \dots J\}$ of the various unknowns of our problem, we deduce their values at time z^{n+1} as follows.

- Computation of p_c^n :

$$\tilde{p}^- = \partial_x^l \tilde{\phi}^-|_{j-1}^n, \quad \tilde{p}^+ = \partial_x^r \tilde{\phi}^+|_{j-1}^n,$$

$$p_c^n = \frac{\tilde{p}^+ + \tilde{p}^-}{2}$$

- Incident wave boundary condition (for $\tilde{\phi}^-$):

$$\tilde{\phi}^-|_1^n = \phi_{inc}(z^n)$$

- Condition on the caustic (for $\tilde{\phi}^+$):

$$\tilde{\phi}^+|_J^n = \phi_c^n$$

- Outgoing boundary condition (on \mathcal{C} for $\tilde{\phi}^-$, on Γ_{inc} for $\tilde{\phi}^+$)

- Computation of $\tilde{\phi}_j^{n+1}$:

$$\tilde{\phi}^\pm|_j^{n+1} = \tilde{\phi}^\pm|_j^n - \delta z \hat{H}(z^n, \tilde{x}_j, u_l^\pm, u_r^\pm)$$

$$u_l^\pm = \partial_x^l \tilde{\phi}^\pm|_j^n, \quad u_r^\pm = \partial_x^r \tilde{\phi}^\pm|_j^n$$

- Computation of x_c^{n+1} :

$$x_c^{n+1} = x_c^n + \delta z H_p(z^n, x_c^n, p_c^n)$$

- Computation of ϕ_c^{n+1} :

$$\phi_c^{n+1} = \phi_c^n + \delta z (p_c^n H_p(z^n, x_c^n, p_c^n) - H(z^n, x_c^n, p_c^n))$$

Increasing order in z

Let us denote by U the set of all our unknowns, and by $U^{n+1} = U^n + \delta z f(U^n)$ the algorithm described above. We use the second order scheme with intermediate step

$$U^{n+\frac{1}{2}} = U^n + \frac{1}{2} \delta z f(U^n)$$

$$U^{n+1} = U^n + \delta z f(U^{n+\frac{1}{2}})$$

4 Numerical results

4.1 Presentation

We conduct a series of experiments with different values of n . In all cases we take $\alpha = \frac{\pi}{4}$ as the angle of \mathbf{e}_b , the direction of the incident plane wave, with the horizontal, i.e.

$$\phi_{inc}(z) = z \sin \alpha$$

We provide two comparisons of these results. First with the Lagrangian ray solution, and when possible with a solution produced with another numerical method [10]. This method only holds for caustics that evolve to the left.

Convergence of the algorithm - ray comparison

The ray solution will be our reference solution. We study the convergence of the algorithm with respect to the location of the caustic, and also compare the values of the phase at the caustic. Let us define the errors made in these computations.

We shoot a dozen of rays. For each, we compute the z coordinate of the point where the ray hits the caustic, by an Lagrangian method [8]. There we evaluate the difference between the position of the ray and $x_c(z)$, and also the difference between the value of the phase transported along the ray by solving (7) and the value of the phase computed by our Eulerian algorithm.

We define the error as the mean value of the errors of each ray. The arrays next section show the behaviors of the errors versus the number of points J used to discretize the x -axis. Due to the limit precision of the ray method (approximately 10^{-4}), the order 1 behavior of the error made in the location of the caustic can only be seen in cases where it keeps away from this limit. In all cases, the convergence of the value of the phase at the caustic is of order 1.

Comparison with the caustic capturing method [10]

We compare the position of the caustic obtained by our method and by another numerical method presented in [10]. This former method only computes the – solution in the case of a caustic evolving towards the inside of the computational domain, but has the particularity to find the exact z -position of the caustic in an asymptotic sense.

Figures

Figures 7 to 18 illustrate the numerical results of our algorithm with $J = 50$ points on the x -axis:

- figures 7, 10, 13, 15, 17 show the contour levels of the phases ϕ^\pm superimposed, and the computed position of the caustic x_c ;

- figures 8, 11, 14, 16, 18 picture the rays together with the position of the caustic we computed;
- in figures 9 and 12, the crosses represent the caustic location computed using the caustic capturing algorithm with a 500 points discretization in space. Our solution is the solid line.

4.2 The numerical experiments

We consider the following z -dependent refraction indexes:

$$n(z, x) = \begin{cases} 1 & \text{if } x \leq 0.5 \\ 1 - (1 + c(z))(x - 0.5)^3 & \end{cases}$$

where

1. $c(z) = 0.2 * z$ – see figures 7, 8, 9.

| Behavior of the errors x e-3 | | | |
|------------------------------|------|------|------|
| J | 25 | 50 | 100 |
| On the caustic | 0.81 | 0.06 | 0.14 |
| On the phase | 10 | 5.8 | 3.1 |

2. $c(z) = 0.05 * z^2$ – see figures 10, 11, 12.

| Behavior of the errors x e-3 | | | |
|------------------------------|-----|------|------|
| J | 25 | 50 | 100 |
| On the caustic | 1.3 | 0.41 | 0.06 |
| On the phase | 12 | 6.4 | 3.4 |

3. $c(z) = -0.05 * z^2$ – see figures 13, 14.

| Behavior of the errors x e-3 | | | |
|------------------------------|-----|-----|------|
| J | 25 | 50 | 100 |
| On the caustic | 2.5 | 1.1 | 0.52 |
| On the phase | 16 | 8.1 | 4.1 |

4. $c(z) = 0.4 * \sin(1.5 * z)$ – see figures 15, 16.

| Behavior of the errors x e-3 | | | |
|------------------------------|-----|-----|-----|
| J | 25 | 50 | 100 |
| On the caustic | 4.7 | 2.2 | 1.0 |
| On the phase | 11 | 6.4 | 3.5 |

5. $c(z) = -0.4 * \sin(1.5 * z)$ – see figures 17, 18.

| Behavior of the errors x e-3 | | | |
|------------------------------|-----|-----|-----|
| J | 25 | 50 | 100 |
| On the caustic | 7.4 | 3.2 | 1.3 |
| On the phase | 15 | 6.9 | 3.5 |

Conclusion

We presented a new method for the direct Eulerian computation of the multivalued solution of Hamilton-Jacobi equation in the case of a fold caustic. We show that the accuracy of the usual method degenerates in the vicinity of the caustic and provided a numerical formula to close our system while maintaining a first order accuracy. This accuracy is required to give a correct boundary condition for the return (+) functions, associated to the part of the rays after the caustic. We also give a systematic initialization procedure of the system when the Cauchy data is only available for the incident wave.

The next step (see [11]) is to compute the transported energy solution of equation (5) and using the solutions ϕ^\pm computed with the algorithm described in this paper.

References

- [1] R. Abgrall. Numerical Discretization of First Order Hamilton Jacobi Equations on Triangular Meshes. *Comm. Pure Appl. Math.* 49 (1996), no. 12, 1339–1373.
- [2] R. Abgrall and J.-D. Benamou. Big ray tracing and Eikonal solver on unstructured grids: Application to the computation of a multi-valued travel-time field in the marmousi model. *Geophysics*, 64:230–239.
- [3] V. I. Arnol'd. *Mathematical methods of Classical Mechanics*. Springer-Verlag, 1978.
- [4] V. I. Arnol'd. *Catastrophe theory*. Springer-Verlag, 1992.
- [5] V. I. Arnol'd, S.M. Gusein-Zade, and A.N. Varchenko. *Singularities of Differential Maps*. Birkhauser, 1986.
- [6] G. Barles. *Solutions de viscosité des équations de Hamilton-Jacobi*. Springer-Verlag, 1994.
- [7] J.-D. Benamou. Big ray tracing: Multi-valued travel time field computation using viscosity solutions of the Eikonal equation. *J. Comp. Physics*, 128:463–474, 1996.
- [8] J.-D. Benamou. Direct solution of multi-valued phase-space solutions for hamilton-jacobi equations. *Comm. Pure Appl. Math.*, 52, 1999.

- [9] J.-D. Benamou and Ph. Montarnal. Equations “géométriques” pour les calcul d’amplitudes d’ondes haute fréquence. *preprint*, 1999.
- [10] J.-D. Benamou and I. Sollicec. An eulerian method for capturing caustics. in *J. Comput. Phys.* 162 (2000), no. 1, 132–163.
- [11] J.-D. Benamou, O. Lafitte, R. Sentis and I. Sollicec. A geometric optics method for high frequency electromagnetic fields computations near fold caustics - Part II. in preparation.
- [12] M. Berry. Rays, wavefronts and phase: a picture book of cusps. In H.K. Kuiken H. Blok, H.A. Fewerda, editor, *Huygens’ Principle 1690-1990: Theory and Applications*. Elsevier, 1992.
- [13] G. Beylkin. Imaging of discontinuities in the inverse scattering problem by inversion of a causal generalized radon transform. *Journal of Mathematical Physics*, 26:99–108, 1985.
- [14] N. Bleistein and S. H. Gray. An extension of the born inversion method to a depth dependent reference profile. *Geophysical Prospecting*, 33:999–1022, 1985.
- [15] Y. Brenier and L. Corrias. A kinetic formulation for multi-branch entropy solutions of scalar conservation laws. *Ann. IHP Analyse non-linéaire*, 1996.
- [16] D. Bouche and F. Molinet *Méthodes asymptotiques en électromagnétisme*. Mathématiques et Applications, vol. 16. Springer-Verlag, 1996.
- [17] H. Cartan. Cours de calcul différentiel. *Hermann, Paris*, 1977.
- [18] M.G. Crandall and P.L. Lions. Viscosity solutions of hamilton-jacobi equations. *Trans. Amer. Math. Soc.*, 277:1–42, 1983.
- [19] M.G. Crandall and P.L. Lions. Two approximation solutions of hamilton-jacobi equations. *Math. Comp.*, 43:1–19, 1984.
- [20] J.J. Duistermaat. Oscillatory integrals, lagrange immersions and unfolding of singularities. *Comm. Pure Appl. Math.*, 27:207–281, 1974.
- [21] B. Engquist, E. Fatemi and S. Osher. Numerical resolution of the high frequency asymptotic expansion of the scalar wave equation. *J. Comp. Physics*, 120:145–155, 1995.
- [22] B. Engquist and O. Runborg. Multi-phase computation in geometrical optics. *J. Comput. Appl. Math.* 74 (1996), no. 1-2, 175–192.
- [23] B. Engquist, O. Runborg and A.-K. Tornberg. High Frequency Wave Propagation by the Segment Projection method. UCLA CAM Report 01-13, 2001.

- [24] M. Fan J. Steinhoff and L. Wang. A new eulerian method for the computation of propagating short acoustic and electromagnetic pulses. *J. Comp. Physics*, 57 (2000), no. 2, 683–706.
- [25] S. Fomel and J.A. Sethian. Fast Phase Space Computation of Multiple Arrival. *preprint*.
- [26] M. V. Fedoryuk. *Partial Differential Equations (Chap. 1)*. Springer-Verlag, 1988.
- [27] F. G. Friedlander. *The wave front set of the solution of a simple initial-boundary problem with glancing rays Math Proc. Camb. Phil. Soc.*, 79-145, 1976.
- [28] I.M. Gelfand and S.V Fomin. *Calculus of Variation*. Prentice-Hall, 1963.
- [29] S. Izumiya. The theory of legendrian unfoldings and first order differential equations. *Proc. Royal Soc. Edinburgh*, 123A:517–532, 1993.
- [30] Izumiya, S.; Kossioris, G. T.; Makrakis, G. N. Multivalued solutions to the Eikonal equation in stratified media. *Quart. Appl. Math.* 59 (2001), no. 2, 365–390
- [31] Katsaounis, T.; Kossioris, G. T.; Makrakis, G. N. Computation of high frequency fields near caustics. *Models Methods Appl. Sci.* 11 (2001), no. 2, 199–228.
- [32] J.B. Keller. A geometrical theory of diffraction. In *Calculus of variations and its applications Vol, 8*. McGraw-Hill, New-York, 1958.
- [33] G. Lambare, P. Lucio, and A. Hanyga. Two dimensional multi-valued traveltime and amplitude maps by uniform sampling of a ray field. *Geophys. J. Int*, 125:584–598, 1996.
- [34] D. Ludwig. Uniform asymptotic expansions at a caustic. *Comm. Pure Appl. Math.*, 19:215–250, 1966.
- [35] B. Merrymann S. Ruuth and S.J. Osher. A fixed grid method for capturing the motion of self-intersecting interfaces and related pdes. *J. Comput. Phys.* 163 (2000), no. 1, 1–21.
- [36] Ph. Montarnal F. Golse, O. Lafitte and R. Sentis. Sur la simulation numérique de la propagation laser. *Rapport CEA*, 1999.
- [37] S. J. Osher and C.W. Shu. High-order essentially nonoscillatory schemes for hamilton-jacobi equations. *SIAM J. Numer. Anal.*, 83:32–78, 1989.
- [38] S. Osher, L.T. Cheng, M. Kang, H. Shim and Y.-H. Tsai. Geometric Optic in a Phase Space Based Level Set and Eulerian Framework. *preprint*.
- [39] P.F. Piserchia, J. Virieux, D. Rodrigues, S. Gaffet and J. Talandier. *A hybrid numerical Modeling of T-Waves propagation: application to the Midplate experiment* *Geophys. J. Int.*, 133 : 3, 789-800. (168) .

-
- [40] O. Runborg. Some new results in multiphase geometrical optics. *M2AN Math. Model. Numer. Anal.* 34 (2000), no. 6, 1203–1231.
 - [41] P. E. Souganidis. Approximation schemes for hamilton-jacobi equations. *J. Differential Equations*, 59:1–43, 1985.
 - [42] W. Symes. A slowness matching algorithm for multiple traveltimes. *TRIP report*, 1996.
 - [43] W. Symes and J.L. Quian. An adaptive finite difference method for traveltime and amplitudes. *TRIP Report Rice U.*, 1999.
 - [44] W. Symes, R. Versteeg, A. Sei, and Q. H. Tran. Kirchhoff simulation migration and inversion using finite-difference traveltimes and amplitudes. *TRIP tech. Report, Rice U.*, 1994.
 - [45] J. Van Trier and W. W. Symes. Upwind finite-difference calculation of traveltimes. *Geophysics*, 56:812–821, 1991.
 - [46] V. Vinje, E. Iversen, and H. Gjoystdal. Traveltime and amplitude estimation using wavefront construction. *Geophysics*, 58:1157–1166, 1993.
 - [47] L.C. Young. *Lecture on the Calculus of Variation and Optimal Control Theory*. 1969.

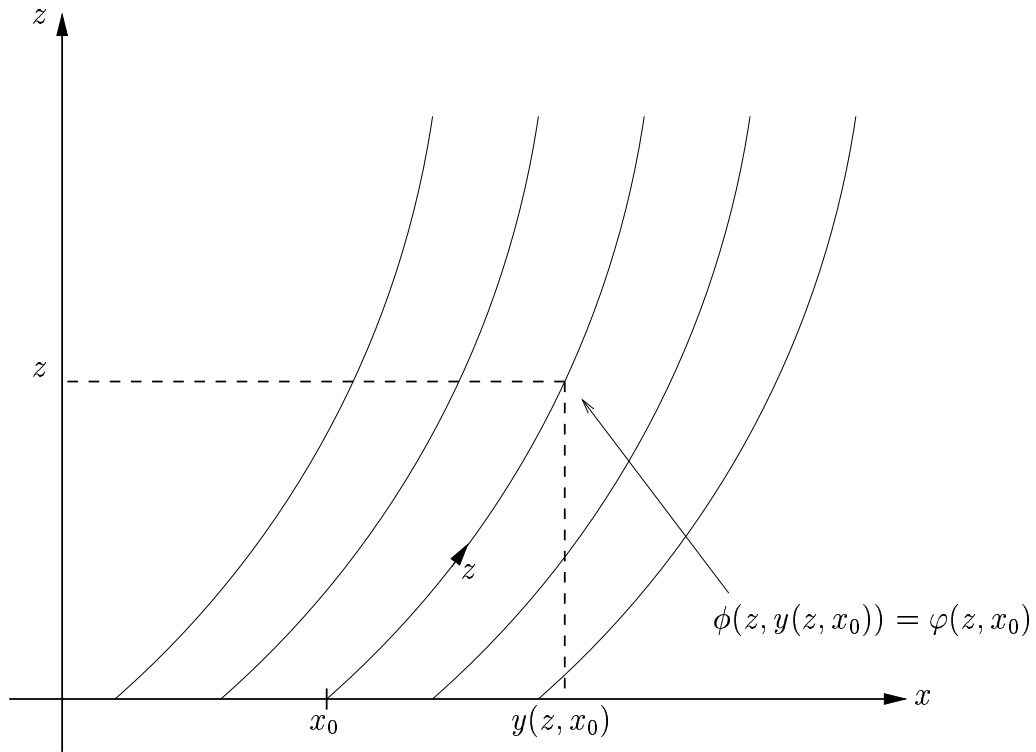


Figure 1: Lagrangian Eulerian correspondance.

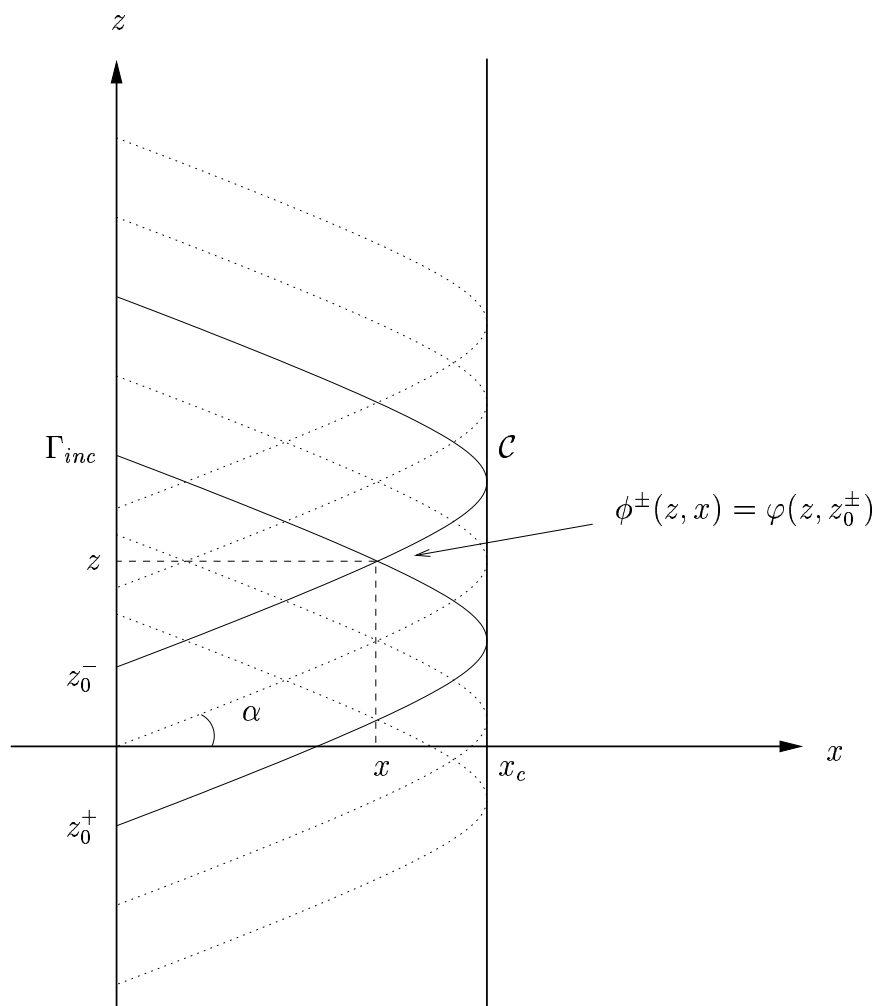


Figure 2: The pseudo-stationary problem.

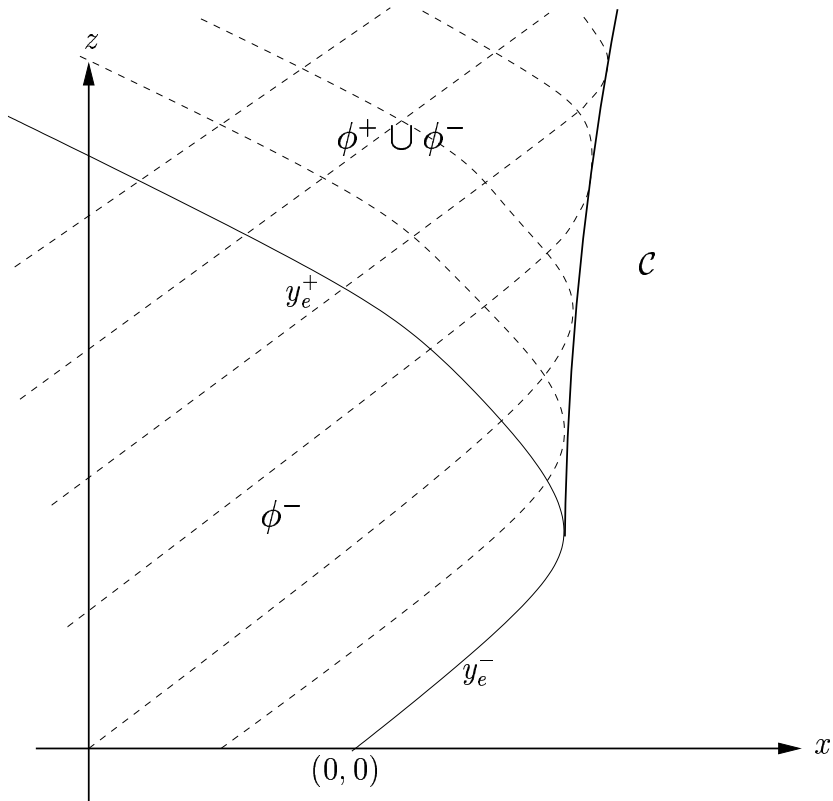


Figure 3: Domains of definition of ϕ^- and ϕ^+ .

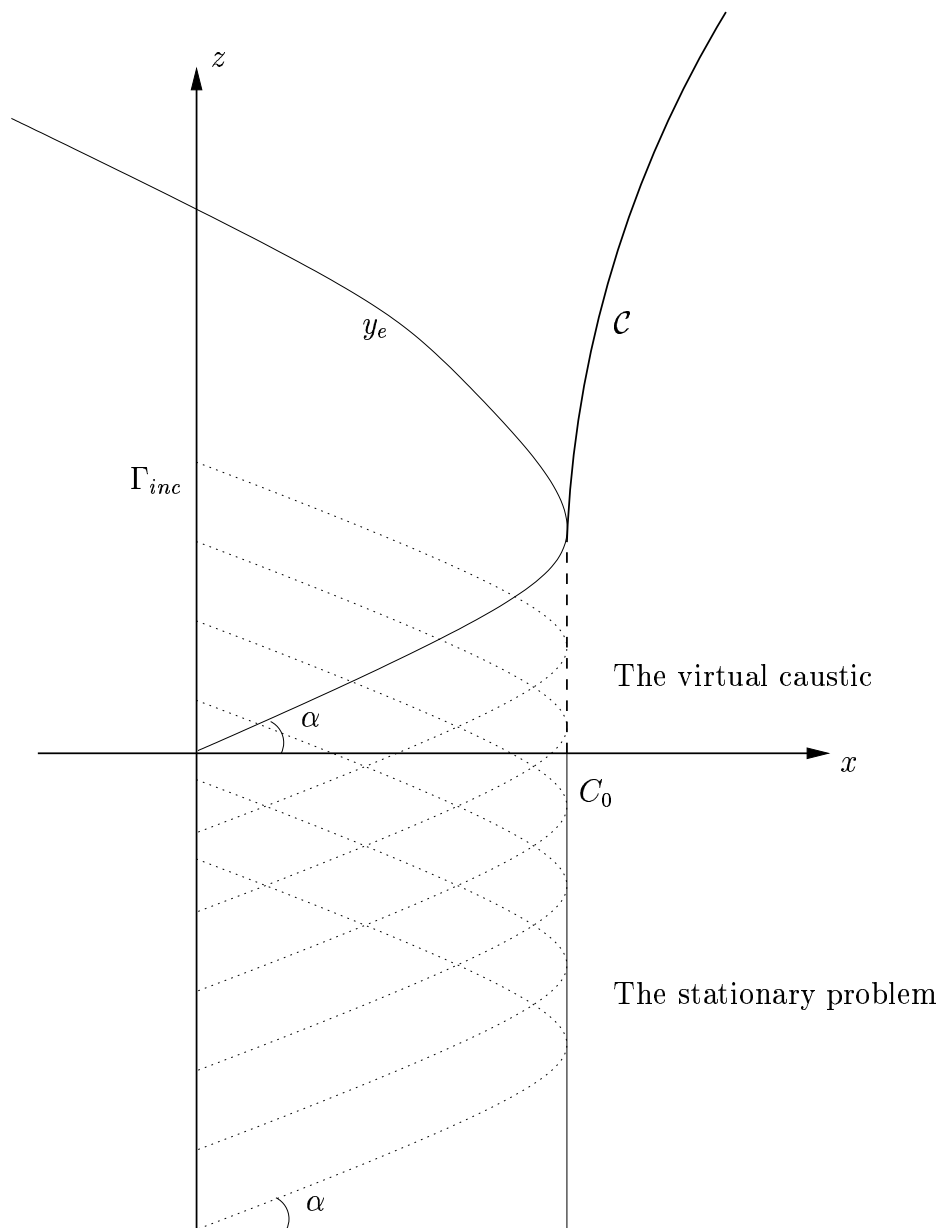


Figure 4: Initialization by a stationary problem.

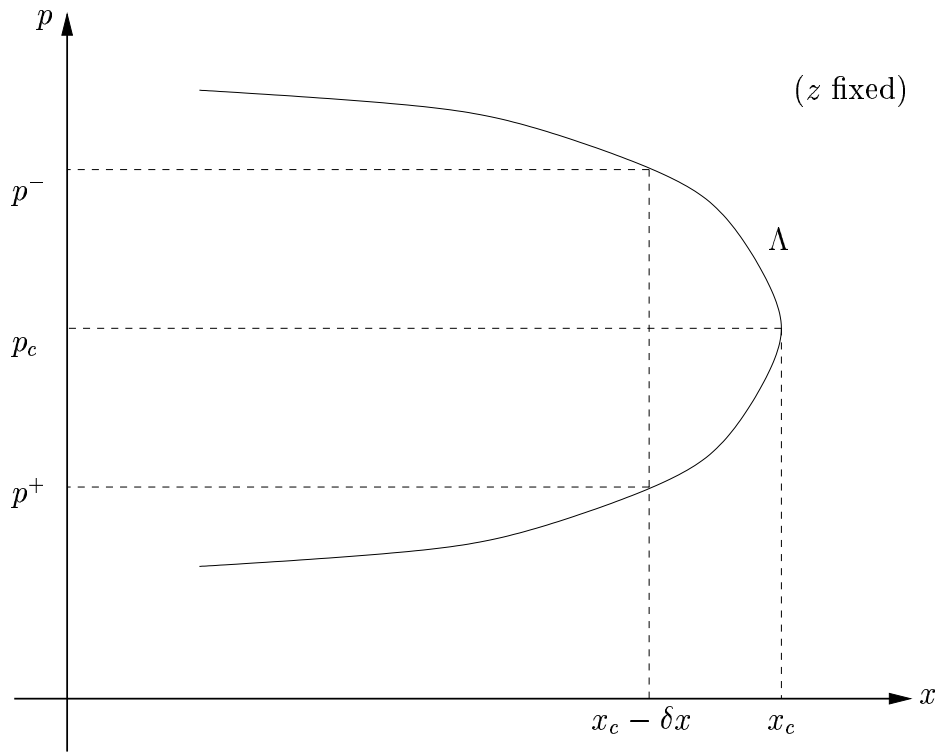


Figure 5: A cut of Λ .

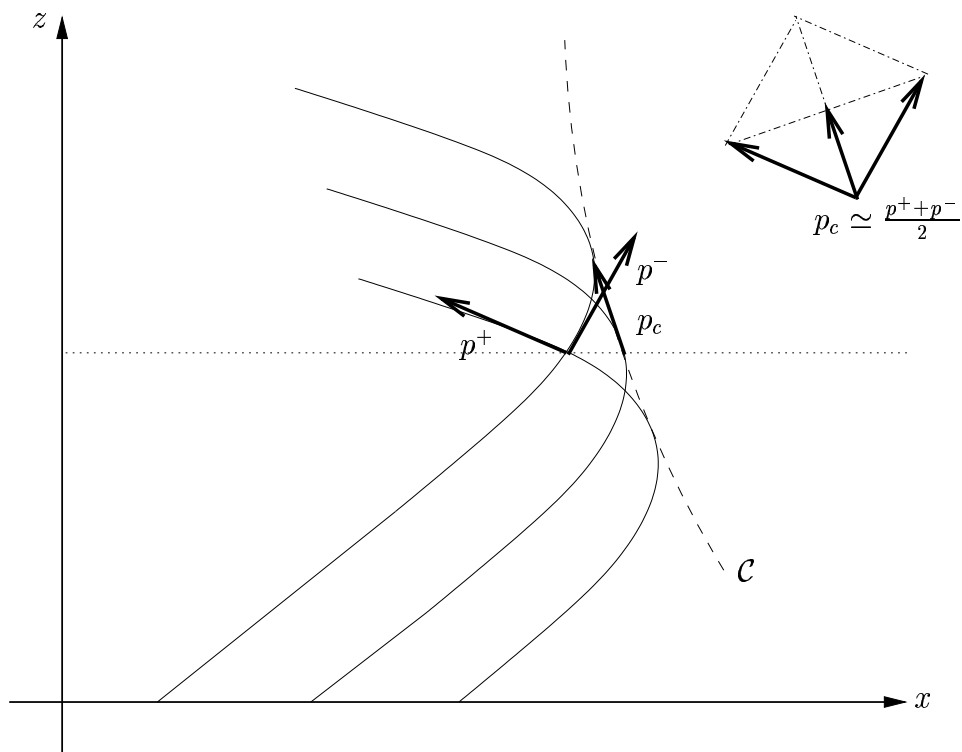


Figure 6: Illustration of formula (37).

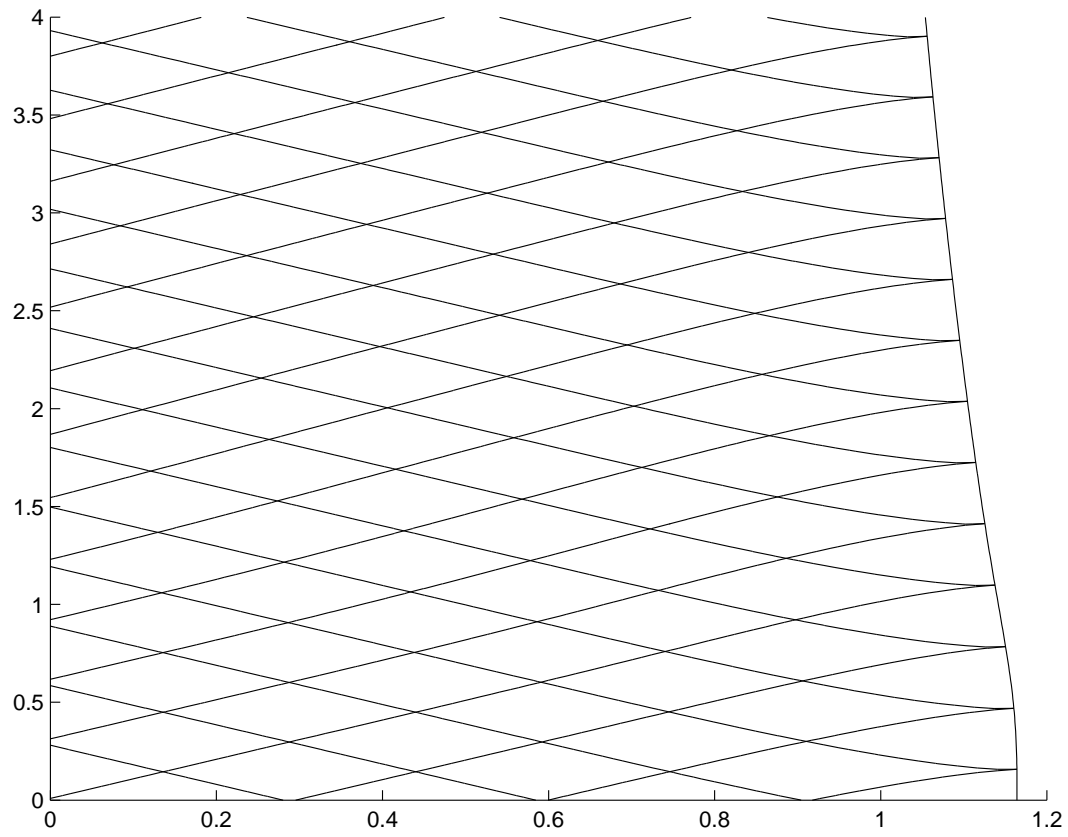


Figure 7: Contour levels of ϕ^\pm – The caustic.

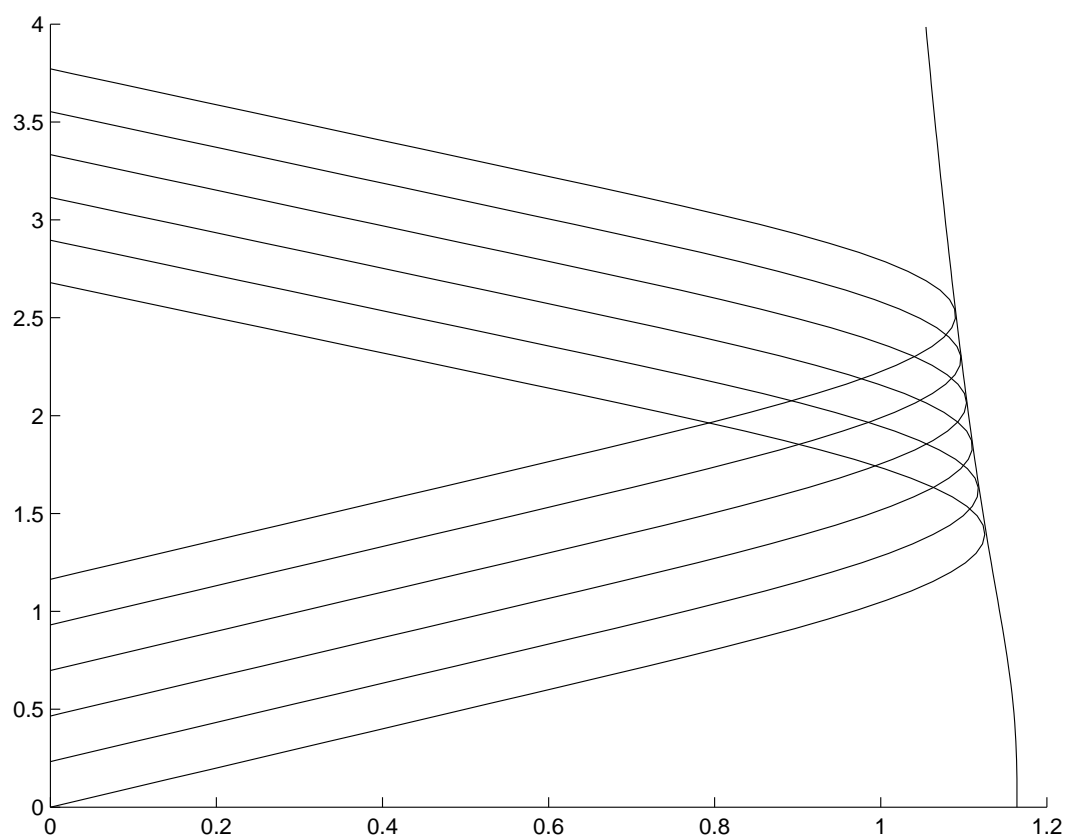


Figure 8: Comparison with the ray method.

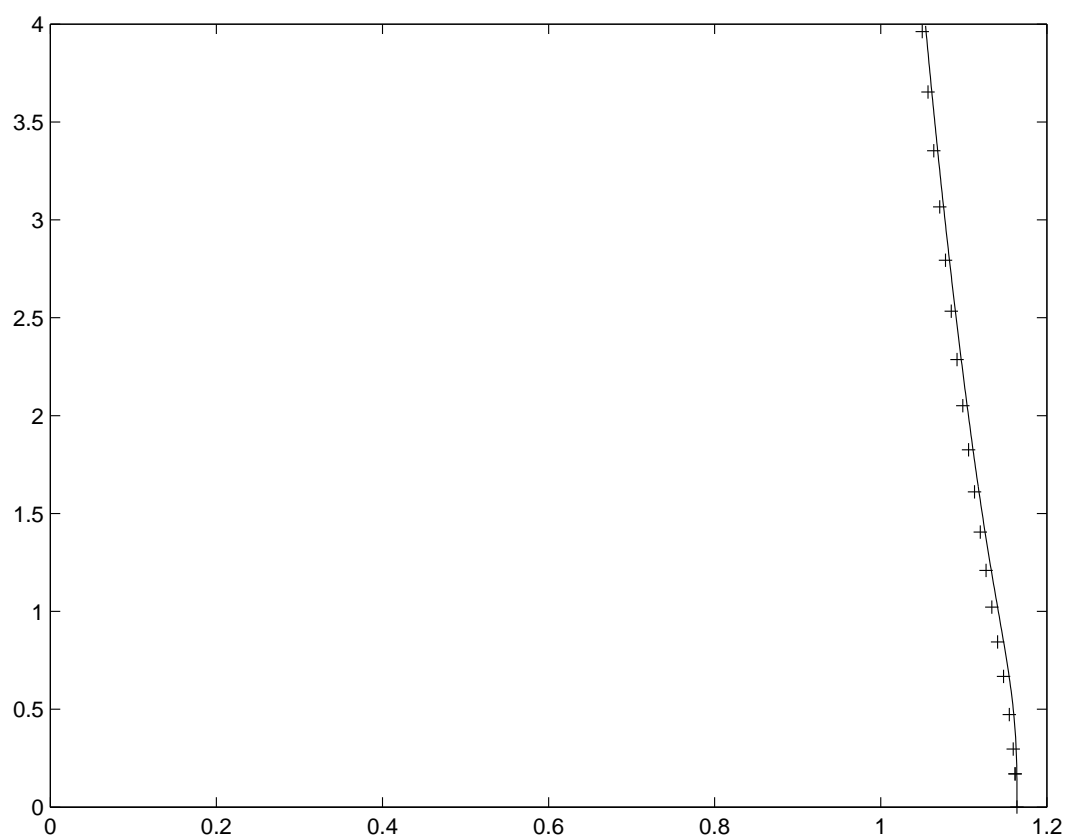


Figure 9: Comparison with the caustic capturing method.

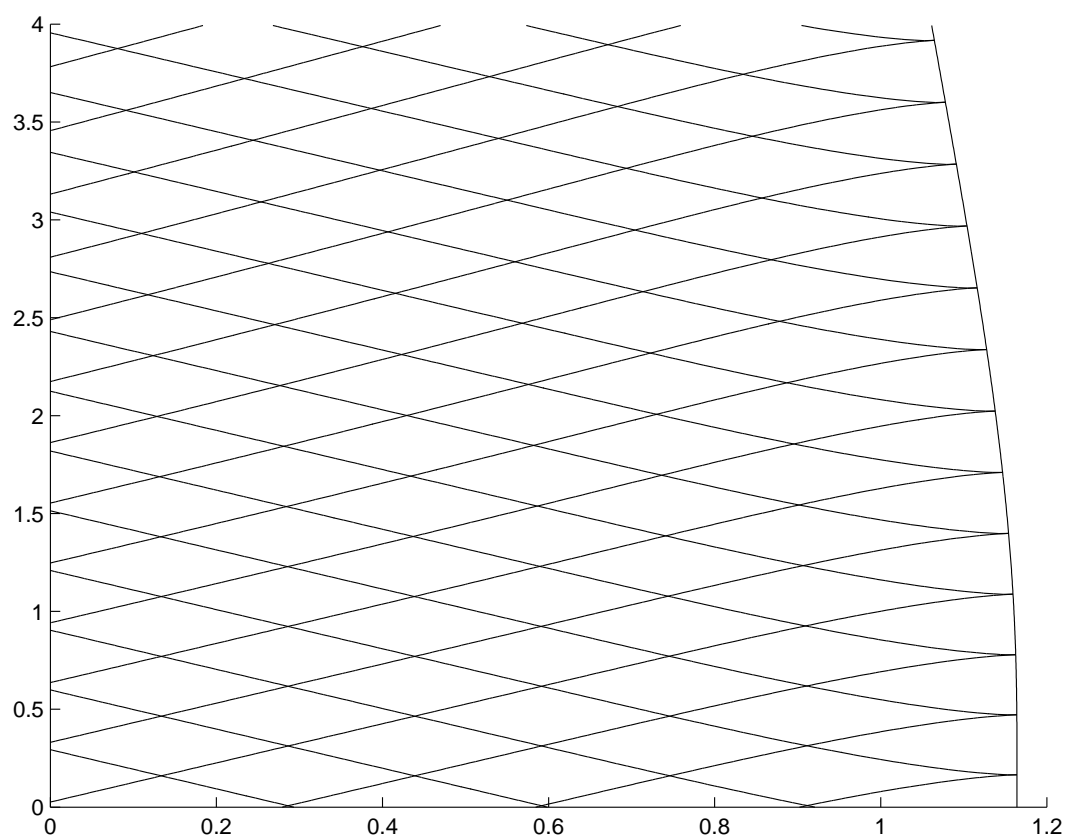


Figure 10: Contour levels of ϕ^\pm – The caustic.

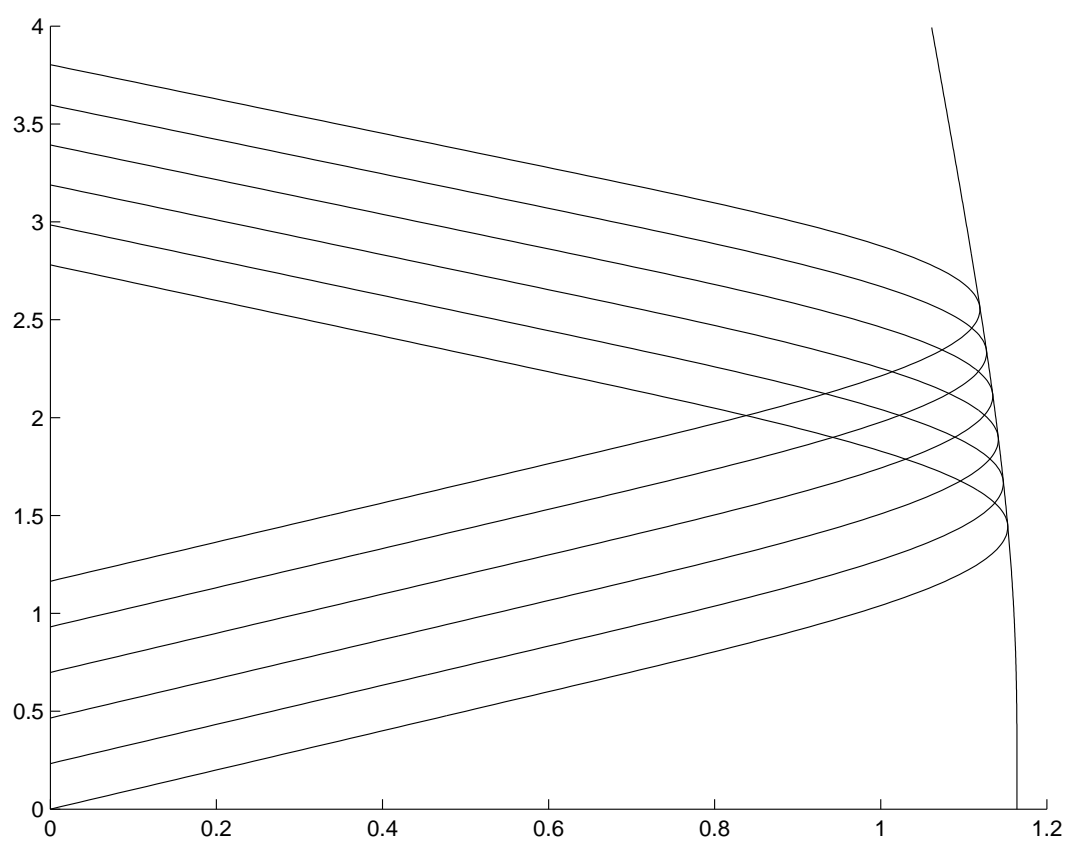


Figure 11: Comparison with the ray method.

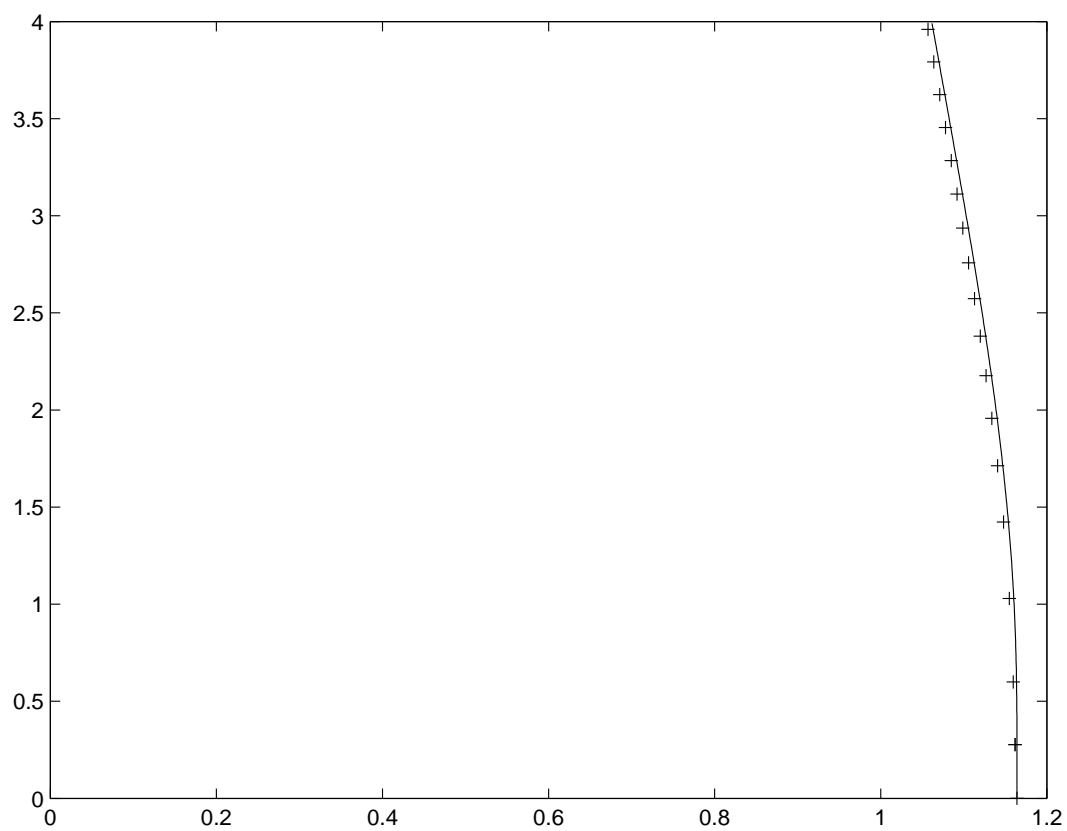


Figure 12: Comparison with the caustic capturing method.

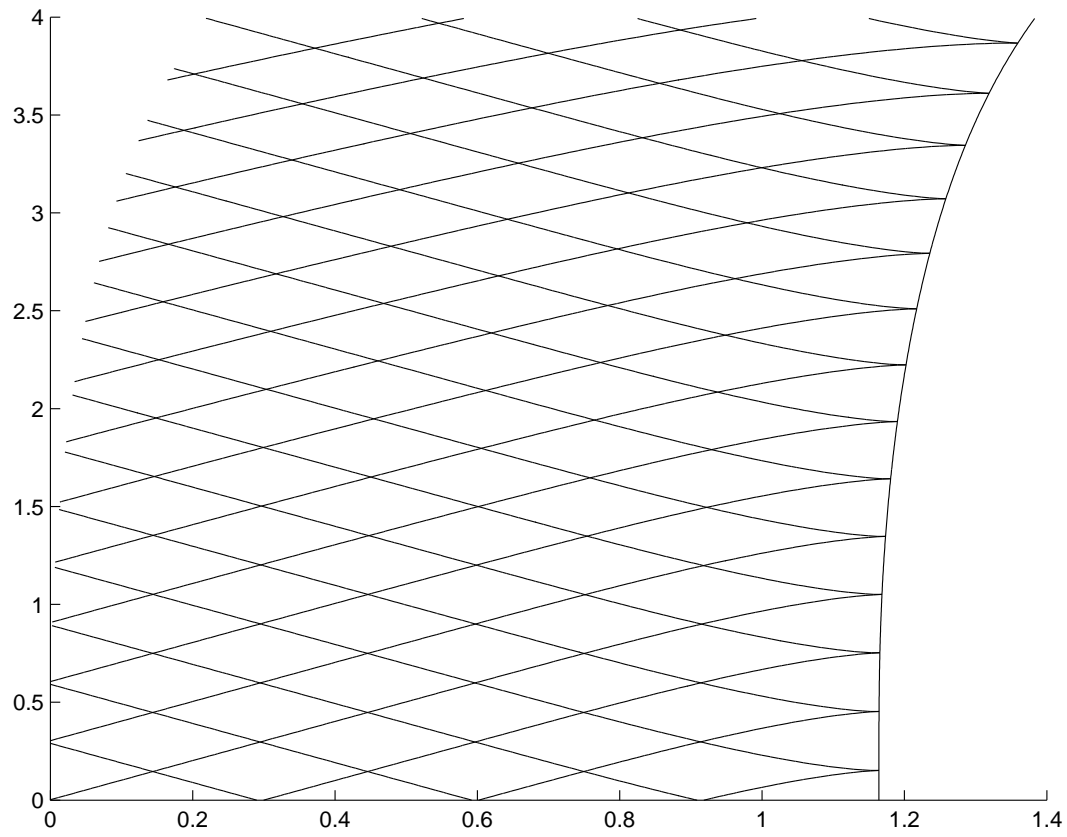


Figure 13: Contour levels of ϕ^\pm – The caustic.

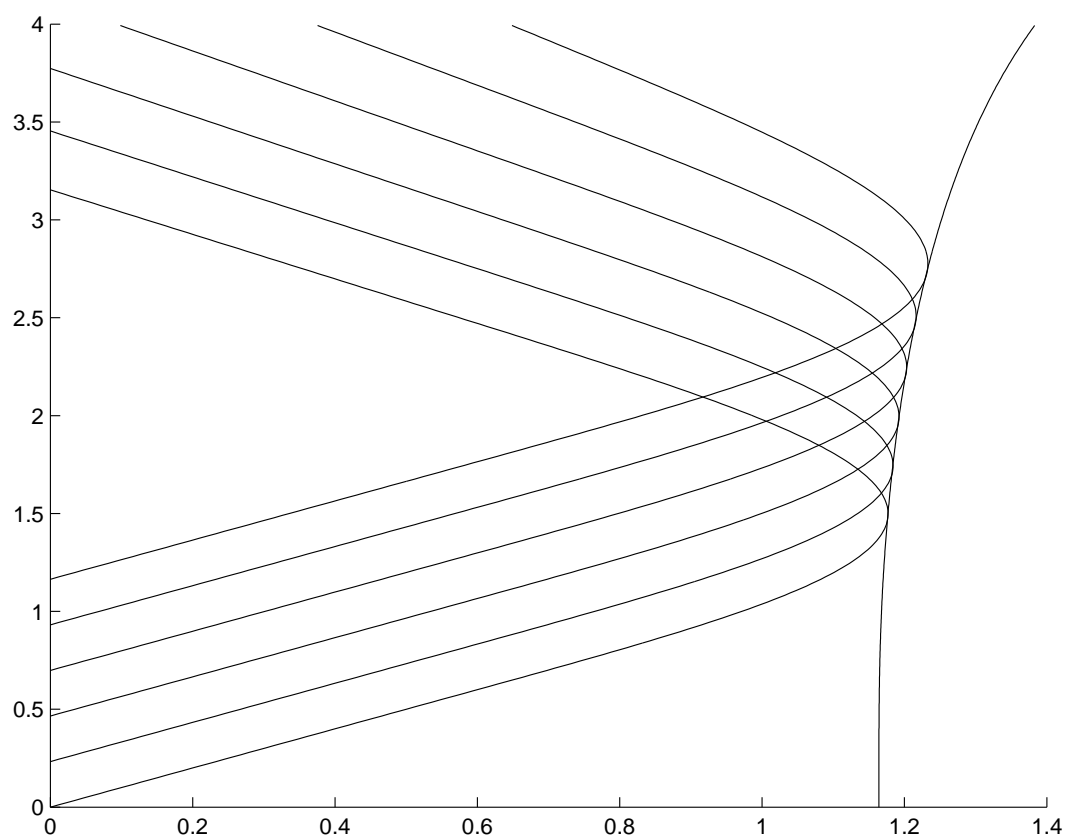


Figure 14: Comparison with the ray method.

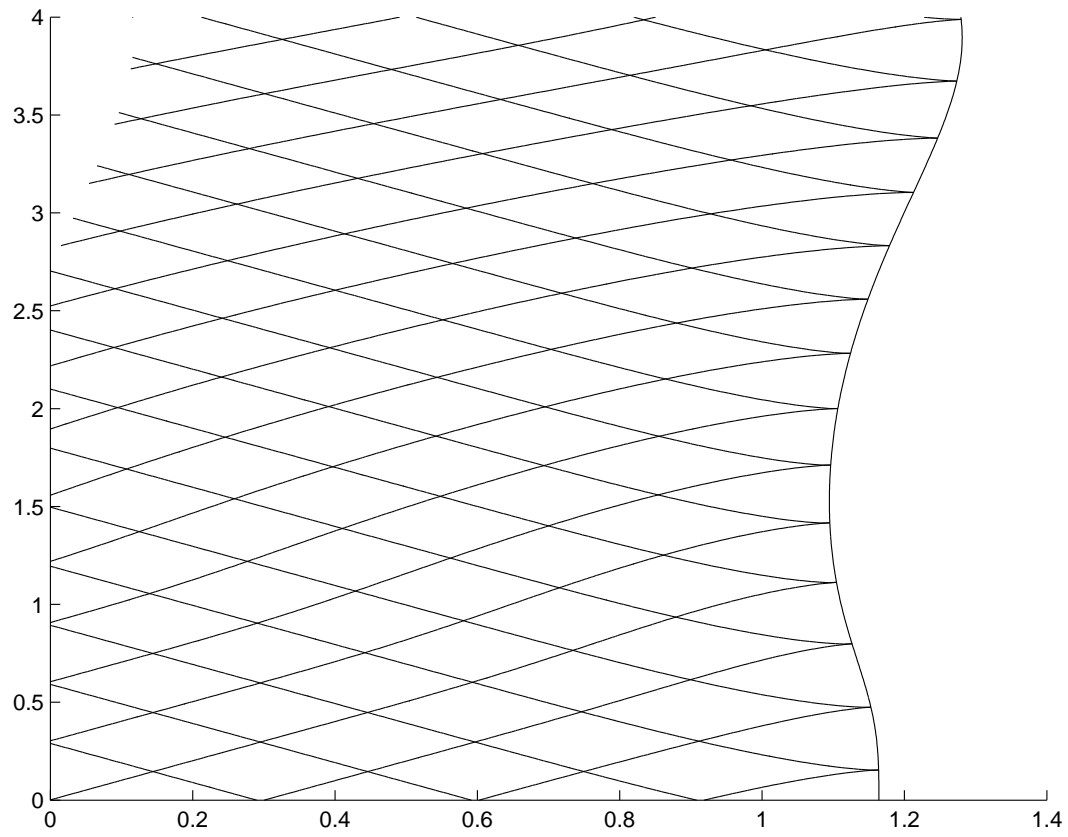


Figure 15: Contour levels of ϕ^\pm – The caustic.

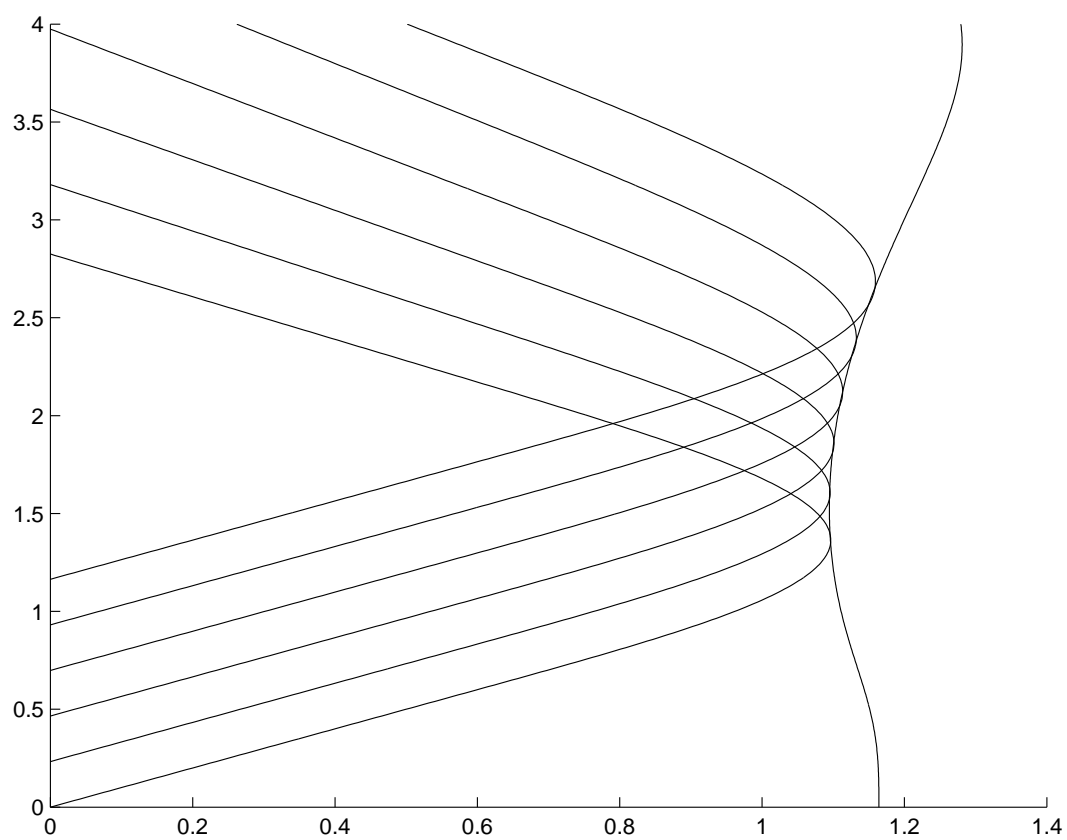


Figure 16: Comparison with the ray method.

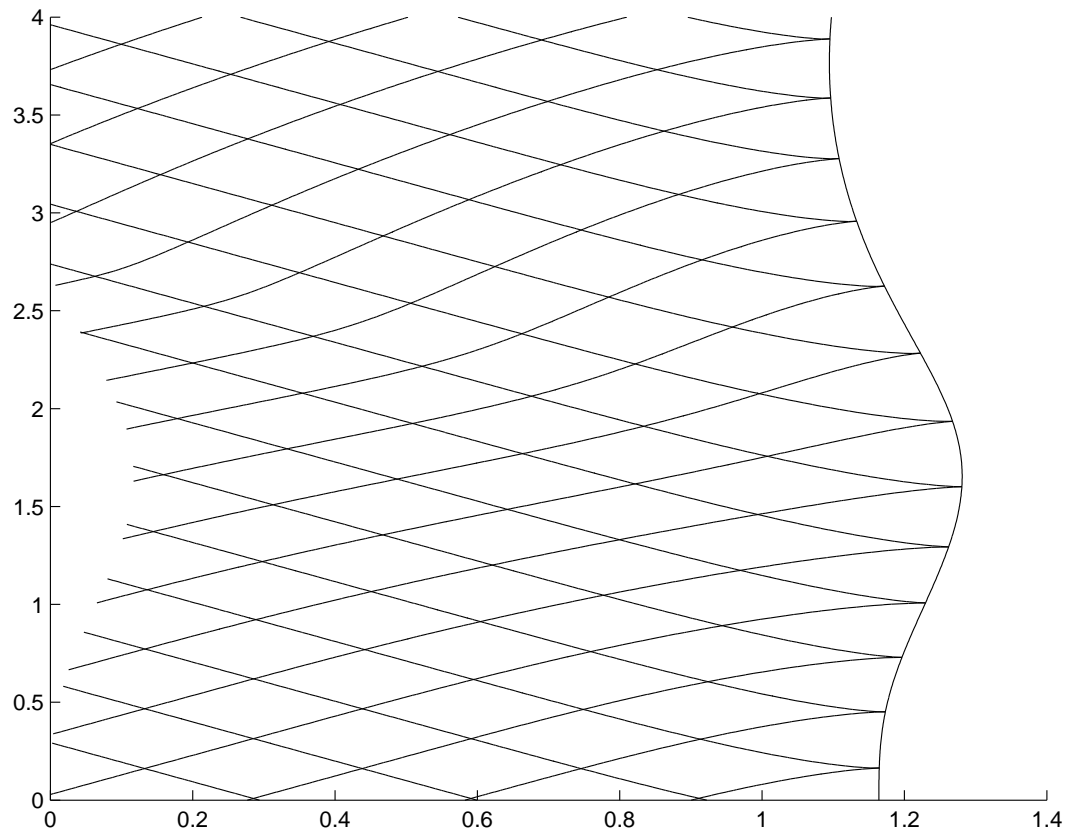


Figure 17: Contour levels of ϕ^\pm – The caustic.

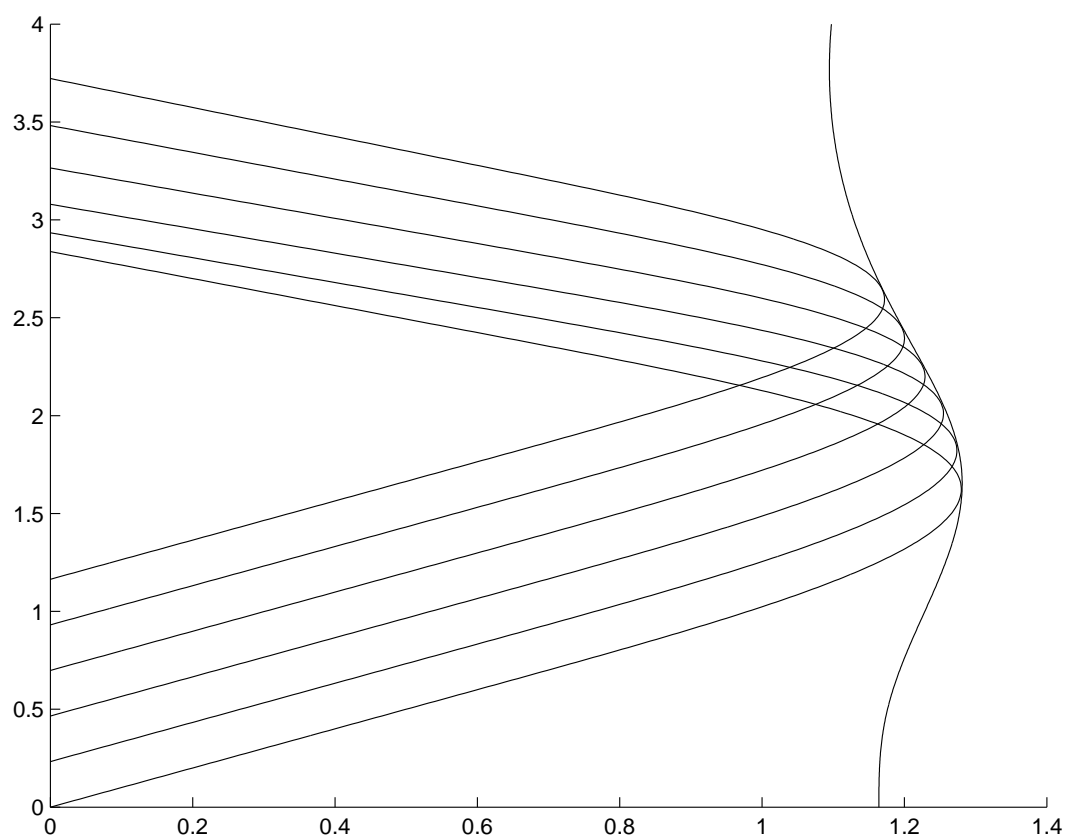


Figure 18: Comparison with the ray method.



Unité de recherche INRIA Rocquencourt
Domaine de Voluceau - Rocquencourt - BP 105 - 78153 Le Chesnay Cedex (France)
Unité de recherche INRIA Lorraine : LORIA, Technopôle de Nancy-Brabois - Campus scientifique
615, rue du Jardin Botanique - BP 101 - 54602 Villers-lès-Nancy Cedex (France)
Unité de recherche INRIA Rennes : IRISA, Campus universitaire de Beaulieu - 35042 Rennes Cedex (France)
Unité de recherche INRIA Rhône-Alpes : 655, avenue de l'Europe - 38330 Montbonnot-St-Martin (France)
Unité de recherche INRIA Sophia Antipolis : 2004, route des Lucioles - BP 93 - 06902 Sophia Antipolis Cedex (France)

Éditeur
INRIA - Domaine de Voluceau - Rocquencourt, BP 105 - 78153 Le Chesnay Cedex (France)
<http://www.inria.fr>
ISSN 0249-6399